CNWRA 2004-04

TEMPERATURE AND RELATIVE HUMIDITY ALONG HEATED DRIFTS WITH AND WITHOUT DRIFT DEGRADATION

Prepared for

U.S. Nuclear Regulatory Commission
Contract NRC–02–02–012

Prepared by

Center for Nuclear Waste Regulatory Analyses
San Antonio, Texas

June 2004

SwRI logo

CNWRA 2004-04

TEMPERATURE AND RELATIVE HUMIDITY ALONG HEATED DRIFTS WITH AND WITHOUT DRIFT DEGRADATION

Prepared for

U.S. Nuclear Regulatory Commission
Contract NRC–02–02–012

Prepared by

R. Fedors
S. Green
D. Walter
G. Adams
D. Farrell
S. Svedeman

Center for Nuclear Waste Regulatory Analyses
San Antonio, Texas

June 2004

ABSTRACT

Estimates of in-drift environmental conditions are used as input to chemical, corrosion, and radionuclide transport models for the potential high-level waste repository at Yucca Mountain, Nevada. This report begins with an assessment of postclosure temperature and relative humidity with and without drift degradation. Estimates are provided for the onset and duration of temperature conditions conducive to localized corrosion of waste packages. Drift degradation delays the onset time of conditions conducive to localized corrosion. Thermohydrological processes reduce the onset time of conditions conducive to localized corrosion. Thus, the effects of drift degradation and thermohydrology need to be factored into performance assessment analyses. Temperature gradients along drifts based on analytical and thermohydrological models are then evaluated to determine the potential areal extent of axial natural convection and to create input for preliminary computational fluid dynamics models of air flow and moisture redistribution in drifts. Simulations using a three-dimensional drift-scale model are used to assess the magnitude of axial air flow along a line of waste packages producing uniform heat loads. Simulation results show that axial flow patterns would not be impeded by the strong cross-sectional flow patterns imparted by the heat rising directly off the waste package, which means axial convection and the cold-trap process will not be limited to the extreme ends of each drift. Also, comparison of results using properties of dry air and water vapor indicate future modeling need not consider changes in fluid (air) properties as a function of vapor content. Simulations of the benchtop laboratory experiments assess the importance of including the moisture model in reproducing realistic values of relative humidity near the heat source. Two ongoing laboratory experiments are briefly described: a condensation cell and a 20-percent scale model of the drift. The U.S. Department of Energy has not decided how natural convection and the cold-trap process will be addressed in any license application for Yucca Mountain as a potential disposal facility for high-level waste. The options are to include the effects of convection and the cold-trap process in performance assessment analyses or to provide a basis for excluding these processes.

CONTENTS

Section Page

ABSTRACT iii
FIGURES vii
TABLES ix
ACKNOWLEDGMENTS xi

1 INTRODUCTION 1-1

1.1 Background 1-2
1.2 Technical Agreements 1-5
1.3 Risk-Informed Aspects 1-6
1.3.1 Waste Package Corrosion 1-6
1.3.2 Transport 1-8
1.3.3 Effect of Drift Degradation 1-8

2 ENVIRONMENTAL CONDITIONS IN DRIFTS 2-1

2.1 Temperature and Relative Humidity 2-2
2.1.1 Temperature Estimates 2-4
2.1.2 Relative Humidity Estimates 2-7
2.1.3 Effect of Thermohydrology on Temperature and Relative Humidity Estimates 2-10
2.1.4 Onset and Duration of Temperature Conditions Conducive to Corrosion 2-11
2.2 Drift-Scale Temperature Gradients in Open Drifts 2-13
2.2.1 Gradients Based on the Conduction-Only Model 2-15
2.2.2 Effect of Thermohydrology on Temperature Gradients 2-18
2.3 Summary 2-20

3 MODELING NATURAL CONVECTION IN HEATED DRIFTS 3-1

3.1 Drift-Scale Simulation with Single Component Gas 3-3
3.1.1 Drift-Scale Model Description 3-3
3.1.2 Drift-Scale Simulation Results 3-4
3.2 Benchtop Experiment Simulation Results 3-6
3.3 Ongoing Laboratory Experiments 3-10
3.3.1 Condensation Cell 3-10
3.3.2 The 20-Percent Scale Experiment of a Drift 3-12
3.3.2.1 The 20-Percent Drift-Scale Design 3-12
3.3.2.2 System Monitoring 3-14
3.4 Summary 3-14

4 CONCLUSIONS 4-1

5 REFERENCES 5-1

APPENDIX

FIGURES

Figure		Page
1-1	Schematic Drawings of (a) Drift Cross Section with In-Drift Water Redistribution, and (b) Drift Segment Showing Axial Air Flow with Short Circuiting	1-5
2-1	(a) Engineered Barrier Components, (b) Radial Approximation, and (c) Schematic of Network for Estimating Temperature from In-Drift Thermal Processes	2-3
2-2	Waste Package Temperature Estimates for Early Degradation, Basecase Degradation, and No Degradation Scenarios	2-5
2-3	Waste Package Temperature Estimates at Center and Edge Locations ... Using Conduction-Only Model Results As the Boundary Condition	2-6
2-4	Temperature Estimates Across the Engineered Barrier System for the (a) Basecase Degradation and (b) No Degradation Scenarios	2-8
2-5	Waste Package Relative Humidity Estimates at Center and Edge Locations of a Drift … Using Conduction-Only Model Results As the Boundary Condition	2-10
2-6	Waste Package Temperature Estimates at the Center and Edge of a Drift for the (a) Basecase Degradation and (b) No Degradation Scenarios	2-12
2-7	Waste Package Relative Humidity Estimates at the Center and Edge Locations … Using Thermohydrological Model Results As the Boundary Condition	2-13
2-8	Estimated (a) Temperature Differences and (b) Local Gradients Along the Eastern Half of a Typical Drift	2-16
2-9	Estimated Portions of the (a) East and (b) West Halves of a Typical Drift with Temperature Differences and Local Gradients	2-17
2-10	Drift-Wall Temperature Estimates from the Two-Dimensional (2D) and Three-Dimensional (3D) Thermohydrological Models	2-19
2-11	Comparison of Drift-Wall Temperature Estimates from the Three-Dimensional (3D) Thermohydrological Model with and without Vapor Phase Lowering	2-21
3-1	Estimated Axial Circulation (Gas Phase) Rate	3-4
3-2	Estimated Axial Fluid (Gas Phase) Temperature Profile	3-5
3-3	Schematic Drawing of Benchtop Cold-Trap Experiment	3-6
3-4	Average Fluid Temperatures Estimated Using FLOW–3D®, with and without Phase Change	3-7
3-5	Estimated Bulk Air and Vapor Flow Rates Using FLOW–3D®, with and without Phase Change	3-8
3-6	Relative Humidity Contour Plot in the Region near the Heater Estimated with Phase Change Using FLOW–3D®	3-9
3-7	(a) Design Schematic of the Condensation Cell. Photographs of (b) Condensation Cell and (c) Water Supply Port and Depression Inside Cell	3-11
3-8	Photographs of the 20-Percent Drift-Scale Natural Convection and Cold-Trap Laboratory Experiment	3-13

TABLES

Table Page

2-1 Onset and Duration of Temperature Conditions Conducive to Localized Corrosion 2-14

ACKNOWLEDGMENTS

This report was prepared to document work performed by the Center for Nuclear Waste Regulatory Analyses (CNWRA) for the U.S. Nuclear Regulatory Commission (NRC) under Contract No. NRC–02–02–012. The activities reported here were performed on behalf of the NRC Office of Nuclear Material Safety and Safeguards, Division of High-Level Waste Repository Safety. The report is an independent product of CNWRA and does not necessarily reflect the views or regulatory position of NRC.

Discussions with F. Dodge and R. Hart contributed to sections of this report and are greatly appreciated. The authors wish to thank C. Manepally for a thorough technical review and useful insights; C. Cudd and B. Long for editorial reviews; R. Mantooth for the format review; and W. Patrick and B. Sagar for programmatic reviews. The administrative and format support provided by P. Houston and L. Selvey is greatly appreciated also.

QUALITY OF DATA, ANALYSES, AND CODE DEVELOPMENT

DATA: Original CNWRA-generated data contained in this report meet quality assurance requirements described in the CNWRA Quality Assurance Manual. Sources for other data should be consulted to determine the level of quality for those data. The work presented in this report is documented in CNWRA Scientific Notebooks 432, 536, and 576.

ANALYSES AND CODES: MULTIFLO Version 1.5.2 code and the commercial package FLOW–3D® Version 8.2 code were used to generate results for this report and are controlled in accordance with the CNWRA software procedure TOP–018.

References:

Flow Science, Inc. "FLOW–3D® User's Manual." Version 8.1.1. Sante Fe, New Mexico: Flow Science, Inc. 2003.

Painter, S., P. Lichtner, and M. Seth. "MULTIFLO User's Manual: Two-Phase Nonisothermal Coupled Thermal-Hydrologic-Chemical Flow Simulator MULTIFLO." Version 1.5. San Antonio, Texas: CNWRA. 2001.

1 INTRODUCTION

Temperature and moisture levels in the drift environment can have a significant influence on waste package integrity at the potential high-level waste repository at Yucca Mountain, Nevada. The effect of heat on moisture movement in the fractured tuff wallrock and in the drifts has historically has been based on porous media model representations. In-drift heat transfer also has been approximated using simplified, analytical expressions for thermal radiation, convection, and conduction. Using these approaches, in-drift temperature and relative humidity estimates along a typical drift are provided. Although useful as current best estimates of temperature and relative humidity, these estimates do not reflect the effects of axial convection, latent heat transfer, and moisture redistribution (e.g., the cold-trap process) in drifts. The direction of ongoing investigations is to gain a better understanding of the combined effect of the thermal processes and moisture redistribution in drifts using laboratory, analytical, and numerical models. Individually, the heat-transfer processes of conduction, convection, radiation, and latent heat are reasonably well understood. The combined effects of all heat-transfer processes in geometrically complex environments, however, are difficult to model. The approach taken in this report is to estimate temperature gradients using analytical heat transfer and thermohydrological porous media models. Then, use those results to constrain two- and three-dimensional computational fluid dynamics models to identify important characteristics of air flow and moisture redistribution patterns that need to be considered in process models and performance assessment.

The need to understand drift-scale {i.e., 1 km [0.6 mi]} and local-scale {i.e., <100 m [330 ft]} temperature variations may be important for performance of the potential repository. Drift-scale temperature gradients may drive axial convection cells that move water in the vapor phase to locations where condensation could occur. Heat transfer caused by natural convection along drifts will affect the onset and duration of environmental conditions conducive to corrosion of the engineered barrier system. Local-scale convection cells affected by the geometric arrangement of the engineered barrier components and emplacement strategy can create zones of reduced temperature, elevated relative humidity, and preferential condensation. Local-scale convection refers to axial and cross-sectional air flow patterns limited to sections of a drift. These air flow patterns can lead to nonuniform temperatures around and between waste packages because of convection beneath the drip shield, around the waste package stand, between individual waste packages, within a rubble pile caused by drift degradation, and between sections of waste packages. Besides variations in temperature caused by the geometrical arrangement of the engineered barrier system, variations in temperature also are caused by differences in heat load between individual waste packages. These local zones around the complex geometry of the engineered barrier system are not addressed in this report, but will be addressed in future studies.

Conductive, thermal radiative, convective, and latent-heat transfer processes all influence temperature estimates in the emplacement drifts of Yucca Mountain. Conduction is important in the solid portions of the engineered barriers and in the wallrock. Radiation is important across air spaces. Convection of air above and below the drip shield will lead to cross-sectional and axial air flow patterns that will enhance heat transfer away from waste packages. The U.S. Department of Energy (DOE) currently incorporates the effects of conductive and convective heat transfers in its total system performance assessment models through the use of effective thermal conductivity in porous media models (CRWMS M&O, 2001a). The convective heat transfer, however, is only incorporated in a radial (cross-sectional sense); that is, no axial

heat transfer or moisture redistribution is incorporated. Although it is clear DOE has begun to assess the effect of the cold-trap process in separate process model calculations (Bechtel SAIC Company, LLC, 2003a,b), the decision to exclude or include moisture redistribution and the cold-trap process as a feature, event, and process in the performance assessment has not yet been made. DOE has not released any report describing their approach or analyses of the effect of natural convection on temperature and moisture distributions in drifts. In preparation for reviewing the bases for the DOE position, the U.S. Nuclear Regulatory Commission (NRC) and Center for Nuclear Waste Regulatory Analyses (CNWRA) have undertaken laboratory and numerical modeling investigations to help understand the significance of natural convection and cold-trap processes on in-drift temperature and moisture distributions.

This report focuses on estimation of in-drift temperature and relative humidity along a typical drift of the potential repository. In Chapter 2, environmental conditions along a typical drift are calculated to support estimates of the onset and duration of conditions conducive to corrosion. The estimates of in-drift temperature and relative humidity reflect the effects of repository edge cooling, thermohydrology, and drift degradation. The estimates, however, only account for natural convection in a radial sense; complex air flow patterns around the engineered barrier system, axial convection, and moisture redistribution are ignored. In Chapter 3, the estimates of temperature along a drift from Chapter 2 are used to provide boundary conditions for computational fluid dynamics models of in-drift air flow. Analyses using the computational fluid dynamics models provide conceptual model support for future modeling of emplacement drifts. In addition, laboratory experiments are described that are intended to support computational fluid dynamics modeling of natural convection and cold-trap processes in drifts.

1.1 Background

Temperature gradients along drifts may drive axial convection cells that move water in the vapor phase to locations where condensation could occur. The edge effect, differential heat loading between sections of a drift, and lithological variations along the drift would all act to create repository-scale temperature gradients. The edge effect is the phenomenon where cooler temperatures are experienced at the ends of drifts relative to the centers because of the influence of the cooler rock beyond the edge of the repository. The particular heat load imposed on a drift is subject to emplacement strategies and different thermal history profiles for various waste types. A possible strategy to lessen the edge effect is to place hot waste packages at the ends of drifts and cool waste packages in the center. No strategy will eliminate temperature gradients entirely, however. Lithological changes affect thermal properties along the drift (e.g., a unit of the Topopah Spring Tuff has larger saturated thermal conductivity that would conduct heat away from the drifts at a faster rate). An approach for estimating temperature gradients along drifts, and the portions of drifts affected by those gradients, was described in Manepally and Fedors (2003). Complementing that approach, this report delves further into the study of large-scale gradients and also focuses on the effect of natural convection on in-drift environmental conditions.

The proposed emplacement of high-level waste in drifts will significantly elevate the temperatures of the drift environment. Temperature gradients along drifts will lead to the movement of air and vapor in natural convection cells. In the cold-trap process, water evaporates at hotter locations, is carried in the vapor phase by convective air flow, and condenses at cooler locations. Elevated relative humidity combined with deliquescence may lead to liquid-phase water contacting waste packages in peripheral zones of the repository

where wallrock temperature may not exceed the boiling point or in internal zones of the repository when the thermal pulse is dissipating. The geometry of the components of the engineered barrier system (e.g., waste package and support, drip shield, and invert) and interaction with the wallrock adds complexity to the problem of simulating air flow and condensation associated with the cold-trap process.

Natural convection and the cold-trap process are expected to modify environmental conditions in drifts from those calculated using models that assume no convection. These modifications potentially could lead to the presence of liquid water and enhanced localized corrosion of some waste packages. For extended periods, benign in-drift conditions are likely to occur. Aggressive conditions, however, may exist in portions of the drifts for shorter periods of time and are dependent on a confluence of temperature, condensation, and chemistry. The waste package outer layer, Alloy 22, may be susceptible to localized corrosion in the presence of liquids with high halide content. The chemistry of water associated with the cold-trap process will differ from that of ambient percolation and thermally refluxed water.[1] The chemistry of condensed water also may vary along the drifts or in the microenvironments of the engineered barrier system because of variations in reactivity with the substrates (e.g., rock bolts, drip shield, and wallrock) on which condensation occurs. Interaction with dust or evaporative residues also will modify the chemistry of the condensate.[2] The cold-trap process will elevate relative humidity in the vicinity of waste packages earlier than the time estimated neglecting convection. The elevation of relative humidity, which may lead to the presence of liquid-phase water, may lead to localized corrosion of waste packages when temperatures are above 80 °C [176 °F] (Dunn, et al., 2003; Brossia, et al., 2001). At this time, the degree to which natural convection and the cold-trap process will modify temperature, relative humidity, and presence of liquid water in drifts, however, cannot be assessed quantitatively with much reliability because of the lack of measured data available to constrain models.

There are two situations where natural convection and the cold-trap process may play a prominent role in repository performance. Cross-sectional flow patterns driven by the heat load from eccentrically located waste packages in the drifts may be strong enough to impede the large-scale axial-flow patterns. The cross-sectional flow patterns also will lead to a nonuniform distribution of temperature around the engineered barrier system. Temperatures on the outside of the waste package are not expected to be uniform because of the combined influence of conduction (to the waste package supports), convection, and thermal radiation. Specific locations where the relative humidity will be elevated near the waste packages, thus increasing the likelihood of condensation, will be controlled by convection in the microenvironments of the engineered barrier system.

Measurements and analyses to support natural convection and the cold-trap process for scales and geometries approaching that of the emplacement drifts are sparse. Temperature gradients, natural convection, and the cold-trap process were cited as a possible cause for the presence of

---

[1]Browning, L., R. Fedors, L. Yang, O. Pensado, R. Pabalan, C. Manepally, and B. Leslie. "Estimated Effects of Temperature-Relative Humidity Variations on the Composition of In-Drift Water in the Potential Nuclear Waste Repository at Yucca Mountain, Nevada." Proceedings of the Scientific Basis for Nuclear Waste Management XXVIII, MRS Spring Meeting, San Francisco, California, April 12–16, 2004. Warrendale, Pennsylvania: Materials Research Society. Submitted for publication (2004).

[2]Ibid.

water puddles, drip marks, and abundant rust on engineered components in the Passive Test of the Enhanced Characterization of the Repository Block drift (Bechtel SAIC Company, LLC, 2003c). Seepage directly into the drift also possibly occurred, although supporting evidence was sparse. Note that seepage as defined by DOE only includes direct dripping, and not along-wall flow or water evaporated from the drift wall (Bechtel SAIC Company, LLC, 2003d). Initial temperature gradients along the Passive Test caused by the episodic operation of the tunnel boring machine were substantially reduced to help assess questions on ambient conditions. After the temperature gradient was substantially reduced, an extensive effort was undertaken to install monitoring equipment in the Passive Test. It is not clear from Bechtel SAIC Company, LLC (2003c) if sparse early measurements or observations in the Passive Test could be used to support numerical models of convection and moisture redistribution. Other measurements that could support models of natural convection and the cold-trap process in heated drifts have not been found in the literature. Ventilated conditions substantially modify processes in drifts, thus data from deep mining operations have not been found to be useful. The Atlas Facility natural convection test (Bechtel SAIC Company, LLC, 2003a) and the Kuehn and Goldstein (1978) analyses of heat transfer support air flow in eccentric cylinders, but were performed at low vapor pressures.

Models for estimating temperature conditions along drifts need to consider mountain, drift, and in-drift processes. Temperature conditions along drifts throughout the potential repository are estimated by DOE using the indirectly linked assemblage of thermal and thermohydrological models at various scales referred to as the Multiscale Thermohydrological Model (CRWMS M&O, 2001a). This assemblage of models is able to estimate temperature gradients along a drift, however, the outer approximately 95 m [310 ft] of most drifts were ignored in the analyses. Temperature gradients may be underestimated if significant portions of the repository edge are outside the outermost thermohydrological model locations. This approach may change in the version of the Multiscale Thermohydrological Model updated for license application. Because of the complex geometry and need to understand air flow and heat transfer associated with natural convection, porous media models of in-drift conditions necessarily rely on other process models for approximating heat transfer in drifts. The cross-sectional (two-dimensional) computational fluid dynamic simulations in Francis, et al. (2003) were used to develop effective thermal conductivity values for the Multiscale Thermohydrological Model. The approach described in Francis, et al. (2003) may provide a glimpse into future DOE modeling of the combined processes of in-drift air flow, heat transfer, and moisture redistribution.

As implied by the discussion above, natural convection and cold-trap processes have been previously discussed in the Yucca Mountain literature (e.g., Wilder, et al., 1996; CRWMS M&O, 2001a; Bechtel SAIC Company, LLC, 2001). The possibility of condensation under the drip shield was cited as the concern (Bechtel SAIC Company, LLC, 2001). Another concern is that condensation on the drip shield and drift wall will migrate to the invert, thus reducing the effectiveness of the drift shaft barrier described by Houseworth, et al. (2003). These moisture redistribution pathways in drifts are illustrated in Figure 1-1. In addition to the moisture redistribution, natural convection will modify temperature distributions along the drift and locally across the engineered barrier system. No analyses of the effect of these processes on in-drift environmental conditions have been provided by DOE. NRC and CNWRA staff have undertaken investigations to help clarify issues associated with effects of natural convection and the cold-trap processes in preparation for reviewing future DOE analyses. Two technical agreements addressing these processes are described in the next section.

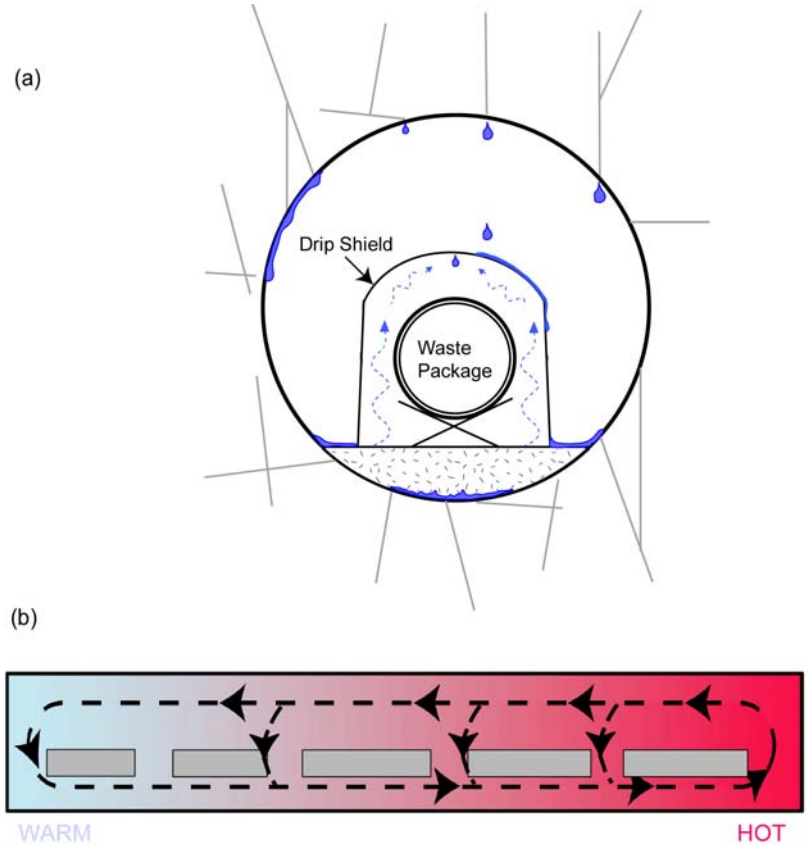

Figure 1-1. Schematic Drawings of (a) Drift Cross Section with In-Drift Water Redistribution, and (b) Drift Segment Showing Axial Air Flow with Short Circuiting; Condensation May Occur Wherever Hot Moist Air Meets Cooler Air or Surfaces

1.2 Technical Agreements

Two NRC and DOE technical agreements were generated about the cold-trap process.

Agreement TEF.2.04: "Provide the Multi-Scale Thermohydrologic Model AMR, Rev. 01. The DOE will provide the Multi-Scale Thermohydrologic Model AMR (ANL–EBS–MD–00049) Rev 01 to the NRC. Expected availability is FY 02."

Agreement TEF.2.05: "Represent the cold-trap effect in the appropriate models or provide the technical basis for exclusion of it in the various scale models (mountain, drift, etc.) considering effects on TEF and other abstraction/models (chemistry). See page 11 of the Open Item (OI) 2 presentation. The DOE will represent the "cold-trap" effect in the Multi-Scale Thermohydrologic Model AMR (ANL–EBS–MD–00049) Rev 01, expected to be available in FY 02. This report will provide technical support for inclusion or exclusion of the cold-trap effect in the various scale models. The analysis will consider thermal effects on flow and the in-drift geochemical environment abstraction."

At the Thermal Effects on Flow Technical Exchange and Management Meeting (Reamer, 2001), the presentation on resolution of the cold-trap process noted DOE would consider the cold-trap effect and would incorporate important effects in the thermohydrological model for performance

assessment. DOE discussed possible approaches for modifying the drift-scale and mountain-scale models. To support these modifications, DOE intended to use a computational fluid dynamics approach for independently assessing heat and mass transfer in the emplacement drifts.

DOE released Bechtel SAIC Company, LLC (2003a), in part, to satisfy technical agreement TEF.2.04. It was not clear from the presented discussion, however, how natural convection and moisture redistribution were incorporated in the Multiscale Thermohydrologic Model or in the Total System Performance Assessment. Or, for an alternative approach, no basis was presented to exclude the cold-trap process and its associated processes of natural convection and moisture redistribution. Bechtel SAIC Company, LLC (2003a) noted a new analysis and model report about natural convection and condensation (Bechtel SAIC Company, LLC, 2003b, draft report) was being developed with an anticipated release date summer 2004. Previously, Civilian Radioactive Waste Management System Management and Operating Contractor (CRWMS M&O) (2001b) concluded that vapor might condense beneath the drip shield, thus warranting additional research on temperature variations caused by natural convection and the cold-trap process. Furthermore, based on simulations using MULTIFLUX, Danko and Bahrami (2004) concluded a significant amount of water will condense along drift segments because of axial convection.

1.3 Risk-Informed Aspects

DOE risk information based on sensitivity studies indicated that factors influencing waste package degradation were important for meeting individual and groundwater protection requirements for the 10,000-year performance period (Bechtel SAIC Company, LLC, 2002). Sensitivity studies of factors influencing in-drift moisture and chemistry were shown to have no effect on mean annual dose. Sensitivity of mean annual dose to rockfall was seen to be significant when mechanical disruption of waste packages occurred.

Creating a closer link between input parameters and issues affecting mean annual dose, NRC (2004) suggested that a number of processes directly influenced by temperature were of high and medium importance for evaluating the DOE performance assessment for the potential repository. NRC (2004) suggested that (i) persistence of passive film on Alloy 22, seepage, and chemistry of seepage water (chemistry of water in drifts) were rated high significance; (ii) effects of accumulated rockfall on engineered barriers, stress corrosion cracking of Alloy 22, and drip shield integrity were rated medium significance; and (iii) invert flow and transport was rated low significance. Temperature conditions in and along drifts will affect chemistry of water contacting the drip shield and waste package, corrosion of waste package and drip shield, and transport of radionuclides through the invert to the unsaturated zone below the drifts. In addition, temperature estimates can be significantly modified when drift degradation and formation of a rubble pile, natural convection, and the cold-trap process are considered.

1.3.1 Waste Package Corrosion

The engineered barrier system includes a waste package with an outer layer of Alloy 22 and a drip shield made of titanium alloy (Bechtel SAIC Company, LLC, 2003e). Before failure, the drip shield will divert liquid water dripping from the drift ceiling. The drip shield may fail because of mechanical deformation caused by rockfall. DOE concludes that general corrosion rates of titanium alloy are low for the estimated conditions of the repository and that localized corrosion

of the titanium alloy need not be considered in performance assessments (Bechtel SAIC Company, LLC, 2003e). Alloy 22 surrounding the waste package may be susceptible to localized corrosion at high temperatures in the presence of saline solutions that only contain small quantities of corrosion inhibitors (e.g., nitrate or sulfate) (Bechtel SAIC Company, LLC, 2003e; Dunn, et al., 2003; Brossia, et al., 2001). Stress corrosion cracking also may occur, if criteria are met for metallurgical susceptibility, corrosive environment, and static tensile stresses. At lower temperatures, when seepage may occur, generalized corrosion can occur and would be dependent on the water flux contacting the drip shield and waste package. Microbially-enhanced localized corrosion also may be a factor, but only at lower temperatures at which microbes can survive. During the performance period, generalized corrosion is not expected to be important, however, the uncertainty of localized corrosion plays a prominent role in the uncertainty of dose (Mohanty, et al., 2002a). From a risk-informed perspective, parameters needed to support inputs to corrosion models include those that quantify factors that affect the onset and duration of the window of susceptibility for localized corrosion of Alloy 22 and the processes by which water contacts the waste containers.

Waste package, drip shield, and drift wall temperature and relative humidity are important parameters for supporting estimates of the amount and chemistry of water contacting waste packages and drip shields, which in turn are input for corrosion models. Because the propagation rate of localized corrosion of Alloy 22 is fast, the time of onset of conditions conducive to corrosion is more important than the duration as long as the duration exceeds specified length of time. Based on parameters in the proposed TPA Version 5.0 code, this length of time is approximately 80 years. Localized corrosion for Alloy 22 is most likely to occur between approximately 80 and 140 °C [176 and 284 °F], when liquid water may occur in dust or residue on the waste package surface.

DOE uses the multiscale thermohydrological assemblage of models to estimate temperature and relative humidity at the waste package, drip shield, and drift wall (Bechtel SAIC Company, LLC, 2003a; CRWMS M&O, 2001a). This model incorporates mountain-scale thermal processes and drift-scale thermohydrological processes. In-drift conditions are approximated with the use of grid cells for air gaps in the thermohydrological model. The effect of natural convection on in-drift heat transfer is approximated in their model, but axial convection and complex cross-sectional flow patterns are ignored. The cold-trap process is neglected in all DOE models.

Using current models, the period encompassing the temperature window has been predicted to span several hundred to several thousand years depending on thermohydrological model inputs and assumptions (Fedors, et al., 2003a; Manepally and Fedors, 2003; CRWMS M&O, 2001a). During the window of localized corrosion, the physical process by which water comes in contact with the waste container must be understood well enough to support estimation of the chemistry of the liquid phase contacting the waste container. Hydrological processes by which water enters and redistributes in drifts, possibly coming in contact with the waste packages, include seepage and dripping, uniform condensation, cold-trap movement of moisture along a drift, and film and rivulet movement of liquid phase water on any in-drift surface (Figure 1-1). Assuming the integrity of the drip shield is maintained, natural convection associated with the cold-trap process could elevate the relative humidity near the waste packages. One possible mechanism to elevate the relative humidity beneath the drip shield is evaporation from the invert. Redistribution of water in the invert and evaporation beneath the waste package may lead to condensation on the underside of the drip shield, followed by dripping onto the waste package.

A dry invert may be rewetted by condensate drainage from the drift wall and drip shield into the invert. Deliquescence enables liquid phase water to form on waste package surfaces at relative humidity values well below the saturated vapor pressure. Because it is an important input to corrosion models, the uncertainty in timing and magnitude of relative humidity in the vicinity of waste packages, with and without considering the effect of the cold-trap process, requires further analysis.

Different modes of water movement lead to different chemical conditions.[3] Evaporated and initially condensated water is relatively dilute and will likely have a low pH. Interaction of the condensed water with the surface material on which it condenses, including any dust or residual mineralization left by previously evaporated water, will alter the chemistry of the liquid phase water.[4] Refluxed water that flows across a residue in fractures of the wallrock likely will be highly concentrated and possibly highly corrosive. NRC will need to evaluate DOE estimates and uncertainty of the relative portions of ambient seepage, refluxed, and condensed water entering the drifts and the effect on chemistry of solutions contacting the waste container.

1.3.2 Transport

Current DOE models predict a dryout zone in the invert and below the drift will serve as a significant natural barrier to radionuclide transport (Bechtel SAIC Company, LLC, 2001). Dripping, along-wall seepage, and condensation from the cold-trap process, however, can accelerate rewetting of the invert in cooler locations. Increased wetness of the invert and the wallrock below the drift will increase radionuclide transport rates if breaching of waste packages occurs. The DOE models used for performance assessment (CRWMS M&O, 2001a) do not currently account for condensation, dripping, and along-wall seepage in the evolution of the drift shadow.

1.3.3 Effect of Drift Degradation

The DOE models for estimating waste package and drift wall temperatures do not include the potential effect of drift degradation and a rubble pile covering the drip shield (Bechtel SAIC Company, LLC, 2003a). If rubble covered the drip shields, large increases in waste package and drip shield temperatures would be expected (Fedors, et al., 2003). DOE estimated that drifts in lithophysal units may collapse and rubble piles may be formed as a result of seismic events (Bechtel SAIC Company, LLC, 2003f). DOE concluded that nonlithophysal units may fail along structural control planes during seismic events on a local basis. DOE does not expect widespread formation of rubble piles covering the drip shield in either lithologic unit.

Current CNWRA estimates of drift degradation based on thermal-mechanical modeling, however, suggest all the repository drifts will likely be backfilled within 1,000 years after closure because of drift degradation processes (Gute, et al., 2003). Drift degradation is modeled as a

---

[3]Browning, L., R. Fedors, L. Yang, O. Pensado, R. Pabalan, C. Manepally, and B. Leslie. "Estimated Effects of Temperature-Relative Humidity Variations on the Composition of In-Drift Water in the Potential Nuclear Waste Repository at Yucca Mountain, Nevada." Proceedings of the Scientific Basis for Nuclear Waste Management XXVIII, MRS Spring Meeting, San Francisco, California, April 12–16, 2004. Warrendale, Pennsylvania: Materials Research Society. Submitted for publication (2004).

[4]Ibid.

stochastic process. Drift degradation will lead to a rubble pile (natural backfill) gradually covering the drip shield during postclosure time. The time when drift degradation starts and the extent of degradation are important parameters for estimating temperatures at the waste package. Fedors, et al. (2003a) described and implemented the approach for linking drift degradation and estimates of temperature. In a sensitivity study, Manepally, et al. (2003) evaluated the importance of some assumptions inherent in the simple network algorithm that linked temperature to drift degradation. Timing and degree of natural backfilling control the magnitude of increased temperatures estimated for the waste packages for the drift degradation scenarios when a rubble pile covers the drip shield.

Convective heat transfer and moisture movement along the length in a backfilled drift will likely be reduced from that in an open drift with only a drip shield. If the drip shield remains intact below the rubble pile, convective heat transfer and moisture movement could occur beneath the drip shield and in the air pocket above the rubble pile. Convection through the rubble pile will likely occur and is expected to be greater than natural convection through the intact fractured wallrock, although it is expected to be much less than that through the open air space of the drift.

Nonuniformity of drift degradation also may increase the local-scale temperature gradients capable of causing increased convective air and moisture transfer along the drift between waste packages or zones of waste packages. Localized zones of degradation may act to bound separate zones of axial convection, with the highest temperatures occurring where rubble piles cover the drip shield. Models of air flow can bound the effects of different drift degradation scenarios without further refinement of geomechanical models (e.g., Gute, et al., 2003). The magnitude of possible convection in the nonuniform drift degradation scenario is not assessed in this report.

2 ENVIRONMENTAL CONDITIONS IN DRIFTS

Containment of radionuclides in the potential repository at Yucca Mountain is dependent on waste package and drip shield integrity. Corrosion of waste packages and drip shields is sensitive to temperature and chemistry of water on their surfaces. In turn, chemistry of water is sensitive to modes of water movement in and near the drifts, which depend on temperature and temperature gradients. Temperature can be considered a primary variable needed to determine which processes and rates to consider for other key technical issues.

To help evaluate U.S. Department of Energy (DOE) estimates of temperature, the Center for Nuclear Waste Regulatory Analyses (CNWRA) has undertaken investigations to assess the importance of drift degradation, repository edge cooling, natural convection, and cold-trap effects on temperature distributions. Drift degradation is expected to lead to increases of in-drift temperatures and delays in the return of liquid water to the drifts (Fedors, et al., 2003); DOE has not evaluated the effect of drift degradation on temperature estimates. Repository edge cooling and natural convection are expected to modify temperature distributions along drifts. Zones in the outer portion of the repository are expected to exhibit conditions conducive to corrosion of waste packages and drip shields sooner than interior zones. Repository edge cooling has been assessed by DOE (CRWMS M&O, 2001a) and Manepally and Fedors (2003), however, natural convection has received little attention. Natural convection and the associated cold-trap process involve temperature gradient-driven air flow with evaporation from warm areas, movement of vapor driven by thermal gradients, and condensation on cool or hygroscopic surfaces. The question then becomes, what temperature gradients may occur in the drifts of a potential repository?

Several combinations of different analytical and numerical thermohydrological porous media models are used in this chapter to

- Estimate in-drift environmental conditions along a drift, specifically temperature and relative humidity, and identify the onset of conditions conducive to localized corrosion of Alloy 22 with and without drift degradation

- Identify extent and timing of significant temperature gradients along drifts to understand the magnitude of areal extent relevant for axial convection

- Estimate temperature boundary conditions along a drift and representative thermal properties of the wallrock for the drift-scale computational fluid dynamics modeling of in-drift natural convection and moisture redistribution described in Chapter 3

This chapter is divided into two parts, one part is about in-drift temperature and relative humidity estimates, and the other part is about in-drift estimates of temperature gradients. In the first part, scenarios with and without drift degradation are considered. In the first section, an abstracted model is used to estimate time-dependent temperature and relative humidity for the repository center and edge locations of a typical drift. Then, results from a detailed thermohydrological model are linked to an in-drift heat transfer algorithm to evaluate temperature estimates previously obtained using the efficient abstracted model. Onset and duration of environmental conditions conducive to localized corrosion are extracted from the temperature and relative humidity estimates for scenarios with and without drift degradation. In the second part, the most computationally efficient model (i.e., conduction-only) for temperature

is used to estimate temperature gradients. Results from a three-dimensional thermohydrological model are used to evaluate the results of the conduction-only model. All results presented in this section are for the postclosure period, but postclosure temperature estimates account for the effect of preclosure forced ventilation using a heat load reduction factor of 0.7 or the time-dependent factors developed by Painter, et al. (2001).

2.1 Temperature and Relative Humidity

An in-drift heat transfer algorithm is used to estimate waste package and drift wall temperatures with and without drift degradation. For the remainder of this report, degradation will always refer to mechanical drift degradation and buildup of a rubble pile on the drip shield. The in-drift heat transfer algorithm uses drift wall temperature estimates provided by either a mountain-scale conduction-only or thermohydrological model. Once the temperature has been estimated, the relative humidity can be estimated using simple assumptions.

For the repository design (DOE, 2002), cylindrical waste packages are to be eccentrically emplaced in a 5.5-m [18.0-ft] diameter drift. The waste packages will be placed on a stand supported by invert material at the bottom of the drift. A drip shield may cover the waste package with air space above and below the drip shield (see Figure 2-1). The effect of drift degradation and formation of a rubble pile covering the drip shield can be factored into an in-drift heat transfer algorithm. This analysis assumes the drip shield remains intact, although the elevated temperatures from natural backfill may affect drip shield mechanical integrity.

The mountain-scale conduction-only model is an analytical, three-dimensional model for heat transfer that uses a line source for a heat load to represent waste packages in each drift. The approach follows the methodology of Claesson and Probert (1996), Carslaw and Jaeger (1959), and a recently submitted proceeding paper.[1] In-drift processes are modeled as conduction (i.e., the drift volume is modeled as an extension of the tuff wallrock). At any one location, the superposition principle is used to combine the effect of heat transfer from all nearby drifts and to approximate the effect of lithologic variations along a drift. Representative effective thermal properties must be used in the conduction model; for example, thermal conductivity varies widely with saturation of the rock, but a single representative value must be used in the conduction equation. An alternative to using temperature estimates from the mountain-scale conduction-only model as the outer boundary condition in the heat transfer algorithm is to use results from the thermohydrological model described in Manepally and Fedors (2003). By linking thermohydrological model results extracted from Manepally and Fedors, improved estimates of waste package temperature are produced because the in-drift heat transfer algorithm approximates the processes of convection and radiation better than the thermohydrological model.

The multimode algorithm for in-drift heat transfer processes is used to estimate waste package surface temperature. The algorithm uses thermal output from the high-level waste (heat load) and wallrock temperature and includes the in-drift thermal processes of thermal radiation,

[1]Mohanty, S., G. Adams, and J. Menchaca. "An Abstracted Model for Estimating Temperature and Relative Humidity in the Potential Repository at Yucca Mountain." Proceedings of the 2004 ASME Heat Transfer/Fluid Engineering Summer Conference, Charlotte, North Carolina, July 11–15, 2004. New York City, New York: AASME. Submitted for publication (2004).

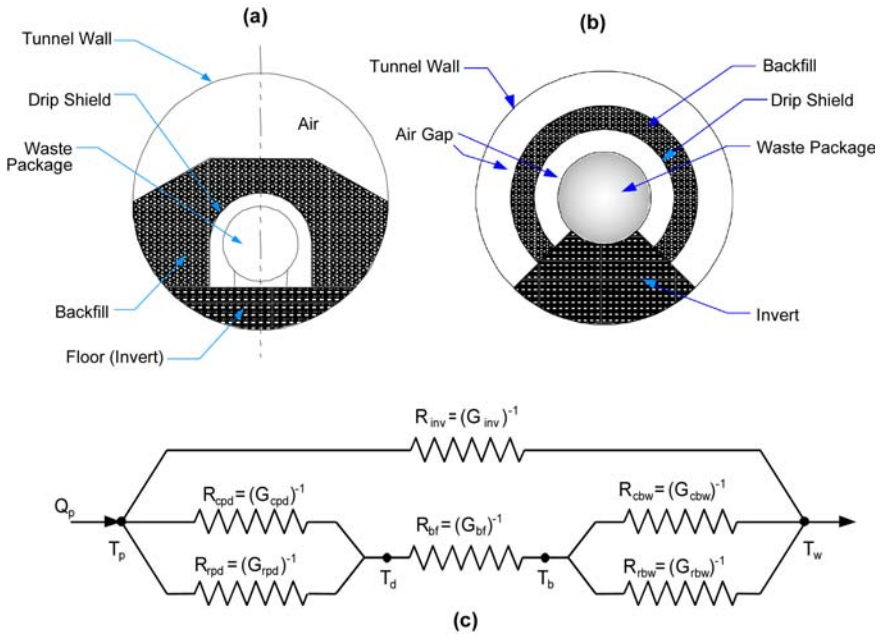

Figure 2-1. (a) Engineered Barrier Components, (b) Radial Approximation, and (c) Schematic of Network for Estimating Temperature from In-Drift Thermal Processes with Linkage to Drift Degradation. R Is the Thermal Resistance, Which Is the Inverse of the Conductance, G.

convection, and conduction. The effect of latent heat transfer is not included in this analysis. The in-drift, multimode algorithm uses the rock temperature estimated either from the conduction-only or thermohydrological model as an outer boundary condition at the drift wall. Hence, mountain-scale processes are decoupled from the in-drift processes. Figure 2-1 shows a schematic of the thermal network algorithm. The multimode algorithm allows fast analyses of new design features or different scenarios.

The multimode algorithm for estimating waste package temperatures is based on the following equation.

$$Q_p = \left[G_{inv} + \left(\frac{1}{G_{cpd} + G_{rpd}} + \frac{1}{G_{bf}} + \frac{1}{G_{cbw} + G_{rbw}} \right)^{-1} \right] \left(T_p - T_w \right) \qquad (2\text{-}1)$$

where

Q_p	—	time-dependent heat supplied by the waste package
G	—	conductance terms
inv	—	invert
cpd	—	convection between the waste package and the drip shield
rpd	—	radiation between the waste package and the drip shield
bf	—	conduction through the natural backfill (if present)

cbw — convection between the drip shield or backfill and the drift wall
rbw — radiation between the drip shield or backfill and the drift wall
T_p — temperature at the waste package
T_w — time-dependent temperature in the rock, outer boundary condition

In Eq. (2-1), T_w is the boundary condition for the in-drift algorithm and is obtained from either the mountain-scale conduction-only model or the thermohydrological model results. Note the value of T_w for the boundary condition in the former case is approximate because it is estimated using the conduction-only model with no drift present. A fraction is assigned that accounts for the portion following the two thermal network pathways—one pathway from the waste package through the invert and one pathway through the airspace, drip shield, and outward. Radial symmetry is assumed (Figure 2-1). Development of expressions for each conductance term for concentric geometries follow the general methodology in Mohanty, et al. (2002b). The expressions for conductance were presented in Fedors, et al. (2003a) and are included in the Appendix of this report for completeness. Whereas heat storage in the wallrock is accounted for explicitly in the estimate of the outer boundary condition, heat storage in the drift is not considered in the equilibrium relation in Eq. (2-1). Slowly changing heat load is assumed to reduce the effect of ignoring in-drift heat storage, particularly for the rubble pile.

The linkage of temperature and drift degradation follows the approach presented in Fedors, et al. (2003a). The in-drift heat transfer algorithm was linked to the drift degradation model of Gute, et al. (2003). Their analyses stochastically estimated the degradation extent for drifts throughout the potential repository. For the analyses presented in this report, the mean drift degradation case leads to a rubble pile that covers the drip shield within 800 years. Parameters in Eq. (2-1) are a function of the height of the degrading drift ceiling and the thickness of the rubble pile, both of which change during time. The air space between the waste package and drift shield remains open for convection, and some air space above the rubble pile may be present. Convection and radiation in the air spaces below the drip shield and above the rubble pile are included in Eq. (2-1). Results for only the postclosure period are presented throughout this report.

2.1.1 Temperature Estimates

Waste package temperature estimates for early degradation, basecase degradation, and no degradation are presented in Figure 2-2. The early degradation scenario is considered an upper bound for temperature estimates. For the early degradation scenario, the drifts are presumed to degrade immediately after closure of the repository. The early, basecase, and no degradation scenarios would lead to peak temperature estimates of 362 °C [684 °F], 236 °C [457 °F], and 171 °C [340 °F]. The more likely scenario would be for nonuniform degradation, thus producing zones of higher and lower temperatures along the drift. The methodology employed in this report is not amenable to simulating the temperature changes along a drift with nonuniform drift degradation. These temperature estimates assume the entire drift uniformly degrades.

Basecase thermal properties from the proposed TPA Version 5.0 code are used in these analyses. Because thermal conductivity varies with saturation, and thus varies spatially and temporally, representative effective thermal conductivity must be used to estimate temporal temperature profiles across the repository. A representative effective thermal conductivity value of 1.59 W/m-K [22.0 BTU/ft-h-°F] is used for the wallrock. The thermal conductivity of the

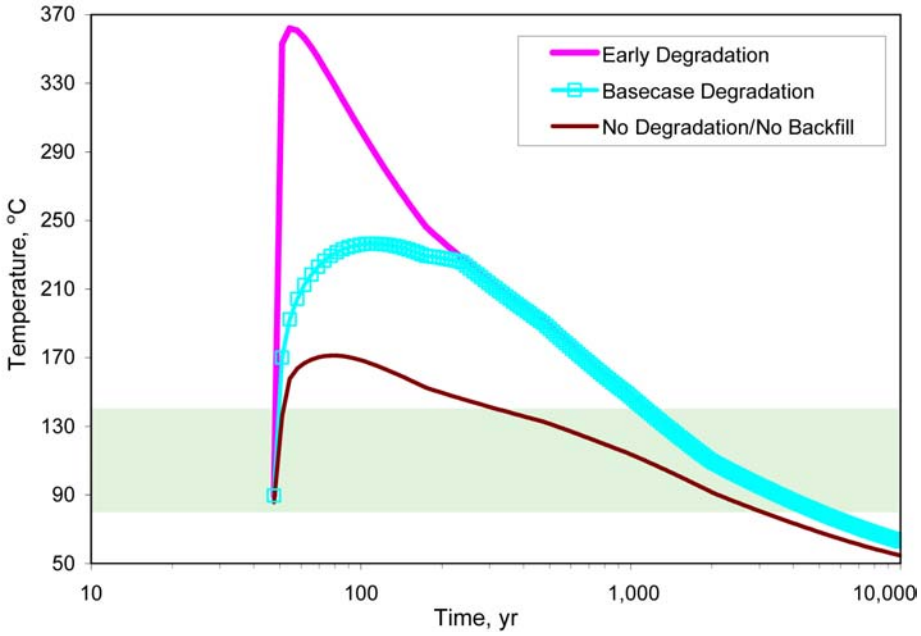

Figure 2-2. Waste Package Temperature Estimates for Early Degradation, Basecase Degradation, and No Degradation Scenarios Using Conduction-Only Model Results as the Boundary Condition for the In-Drift Heat Transfer Algorithm. Shaded Area Marks Zone of Temperature Conditions Conducive to Corrosion [°F = (1.8 × T °C + 32)].

rubble, however, is not yet part of the proposed TPA Version 5.0 code (Mohanty, et al., 2002b). A representative effective thermal conductivity value of 0.27 W/m-K [3.75 BTU/ft-h-°F] is used for the analyses presented in this report based on the value used for the invert in the proposed TPA Version 5.0 code basecase. Fedors, et al. (2003a) and Manepally, et al. (2003) showed there was a large sensitivity of temperature to the thermal conductivity value used for the rubble pile. The thermal conductivity value for the rubble pile is highly uncertain; no supporting basis has been found in the general literature.

Temperature as a function of time at the center of the repository does not reflect adequately the environmental conditions along drifts. Figure 2-3 illustrates the bounding waste package temperature profiles for a drift; all temperature conditions between the profiles (center and edge) occur at some location along the drift. The host rock properties are assumed constant along the drift for these estimates of the temperature profile. For the basecase degradation scenario (Figure 2-3a), temperature estimates for the east and west ends of the drift are nearly identical because conduction through the rubble pile dominates the heat transfer in the system.

The center and edge profiles are said to bound the conditions in a drift because, if profiles for every location were plotted in Figure 2-3, the curves would completely populate the zone between the center and edge temperature profiles. For example, at the peak temperature in the drift degradation scenario, there is a temperature range along the drift from 150 °C [302 °F] at the edge to 236 °C [457 °F] at the center. Similarly at 1,000 years, there is a temperature range along the drift from 97 °C [207 °F] at the edge to 146 °C [295 °F] at the center. Thus, there is a zone of the drift where temperature conditions are conducive to localized corrosion early in the performance period that would be missed if the center location was considered representative

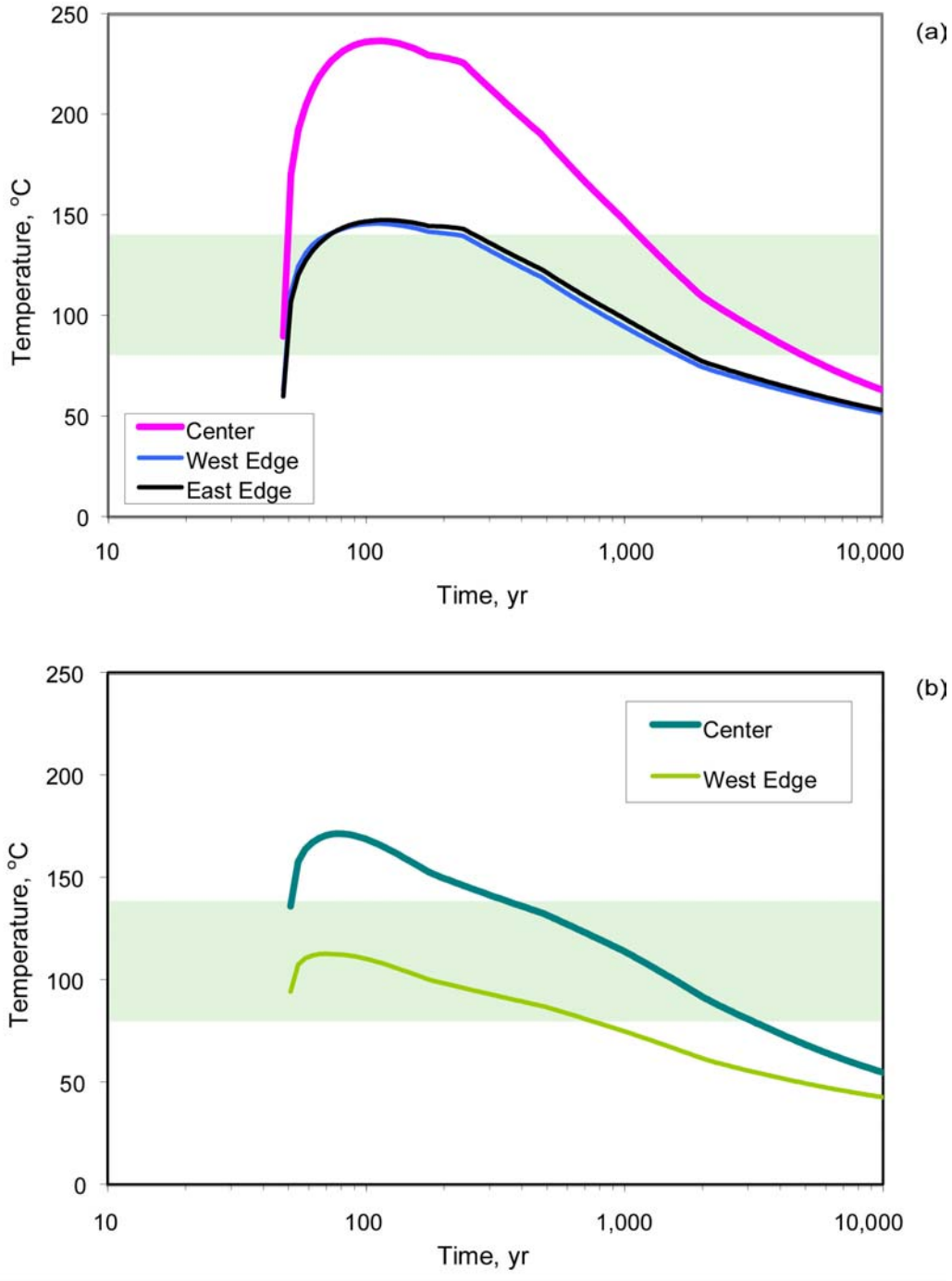

Figure 2-3. Waste Package Temperature Estimates at Center and Edge Locations for (a) Basecase Degradation and (b) No Degradation Scenarios Using Conduction-Only Model Results As the Boundary Condition for the In-Drift Heat Transfer Algorithm. Shaded Areas Mark Zone of Temperature Conditions Conducive to Corrosion [°F = (1.8 × T °C + 32)].

of the entire repository. Similarly, there is a portion of drift at all times between 50 and 3,000 years for the no degradation scenario (Figure 2-3b) when the conditions are conducive to localized corrosion of Alloy 22.

The basecase degradation and no degradation scenarios lead to markedly different temperature profiles across the engineered barrier system and into the wallrock. For the no degradation scenario, radiation and natural convection are effective and efficient for transferring heat from the waste package to the wallrock. Estimates of temperature differences between the waste package and the wallrock are approximately 10 °C [18 °F] for the no degradation scenario at the time of peak temperature. This temperature difference decreases as the thermal pulse dissipates.

For the degradation scenario, there are large temperature differences between the waste package and the drift wall. Figure 2-4 illustrates the temperature profile across the engineered barrier system at a center location. The temperature difference of 86 °C [187 °F] between the waste package and the drift wall at approximately 113 years illustrates how conduction through the rubble pile dominates the estimate of temperature in the basecase degradation scenario. As will be shown in the next section, the large temperature difference in the basecase degradation scenario keeps the relative humidity low near the waste package. Once the boiling isotherm passes through the rubble pile, however, increased capillarity caused by fines (rock dust) settling in the rubble pile will lead to enhanced levels of moisture in contact with the drip shield or waste package.

2.1.2 Relative Humidity Estimates

Relative humidity, along with temperature and chemistry of water and dust or residue on waste package surfaces, is used to assess the potential for localized corrosion of Alloy 22 (Bechtel SAIC Company, LLC, 2003a,e; Dunn, et al. 2003). At relative humidity fractions less than one, but greater than the deliquescence point, dust or residue on the waste package surface can draw moisture out of the gas phase and form liquid phase water as brines on the material surface. The relative humidity value at which liquid water may occur, called the deliquescence point, depends on the chemical composition of the dust or residue.

The temperature difference between the waste package and the drift wall is an important factor for estimating relative humidity at the waste package. The temperature of the drift wall also is important because the supply of water comes from the drift wall (assuming no in-drift moisture redistribution due to axial convection). The estimate of relative humidity near the waste package assumes well-mixed air in the drift and uses the drift wall and waste package temperatures. The calculation of relative humidity depends on whether the temperature of the drift wall is above or below boiling.

Below boiling, the relative humidity is defined as the actual mole fraction of water vapor in the air divided by the mole fraction when the air is saturated with water vapor at the same temperature. For above boiling conditions, it is assumed vapor partial pressures cannot exceed the atmospheric pressure in drifts (i.e., there is no pressure buildup in the heated drifts). Thus, for above boiling, it is assumed the amount of water vapor held in the air phase at the boiling temperature remains constant for all temperatures above the boiling temperature. Also, by definition, the relative humidity has to be 100 percent at the boiling temperature for pure water not held by capillary tension.

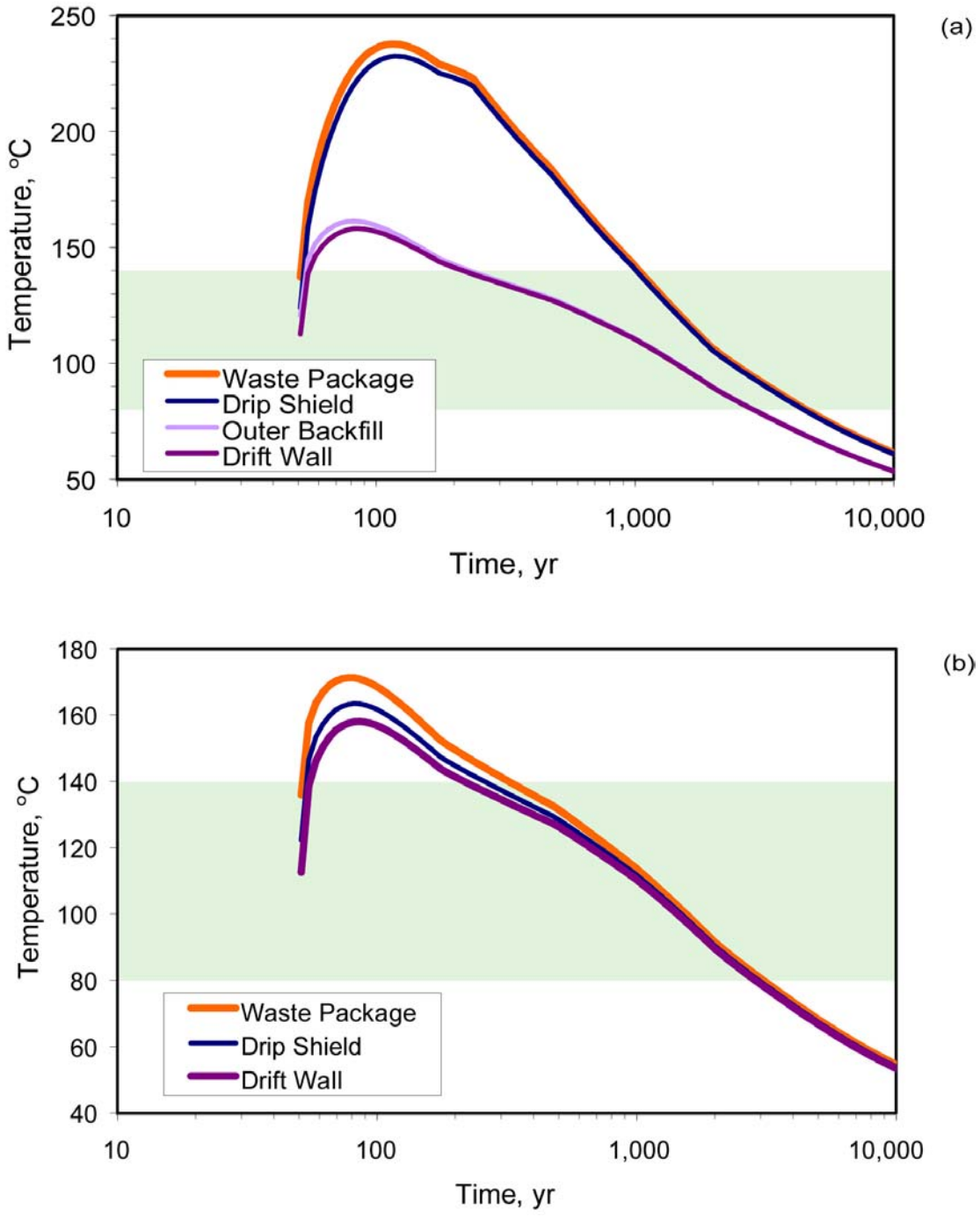

Figure 2-4. Temperature Estimates Across the Engineered Barrier System for the (a) Basecase Degradation and (b) No Degradation Scenarios Using Conduction-Only Model Results As the Boundary Condition for the In-Drift Heat Transfer Algorithm. Shaded Areas Mark Zone of Temperature Conditions Conducive to Corrosion [°F = (1.8 × T °C + 32)].

At the elevation of the repository, total pressure dictates the boiling temperature is between 96 and 97 °C [204.8 and 206.6 °F]. The assumptions are that capillarity does not affect the boiling temperature, and pore water is pure water. Capillarity and high concentrations of ions in solution will serve to elevate the boiling point temperature estimated for the drift wall. Higher boiling point temperatures at the drift wall will increase estimates of relative humidity for above-boiling conditions. Theoretical hydrology dictates that capillarity force competes with the phase change for boiling, thus lowering the vapor phase pressure (and hence relative humidity). Chemists define relative humidity as the lowering of vapor pressure caused by ions (Pabalan, et al., 2002). This vapor pressure lowering is called the deliquescence. Similar to vapor pressure lowering by capillary forces, the chemist definition implies the gas phase is holding the maximum amount of moisture it can physically hold (i.e., it is saturated with respect to water). Liquid phase solutions on a surface will exist at relative humidity values above the deliquescence point.

In the drift environment, relative humidity is estimated for the basecase degradation and the no degradation scenarios using two simple assumptions. The first assumption pertains to the definition of relative humidity above the boiling temperature. The estimate of relative humidity uses a ratio of saturated vapor pressures with the numerator dependent on the temperature at the drift wall. The denominator for this definition of relative humidity is always the saturated vapor pressure at the temperature of the waste package. Saturated pressures of water vapor are approximated using the Keenan, Keyes, Hill, and Moore formula (American Society of Heating Refrigeration and Air Conditioning Engineers, Inc., 1977). If the temperature at the drift wall is below boiling, the numerator is the saturated vapor pressure at the temperature of the drift wall. If the temperature at the drift wall is above boiling, the numerator is the saturated vapor pressure at boiling. Intuitively, this definition of relative humidity is reasonable because at boiling, the relative humidity is 100 percent. Above boiling, no additional water can enter the gas phase because the vapor pressure cannot exceed the total pressure, which remains at the local atmospheric pressure. Hence, the moisture content of the gas phase remains constant for all temperatures above boiling.

For the second assumption, the rubble pile is expected to contain large open-space voids through which the resistance to air flow is considered negligible. In essence, the rubble pile still allows for a well-mixed gas phase throughout the drift opening.

Relative humidity estimates for the center and edge locations are plotted in Figure 2-5 for the basecase degradation and no degradation scenarios. With drift degradation, estimates of relative humidity values are lower and remain lower much longer than those of the no degradation scenario. For the no degradation scenario, the relative humidity values revert to high values (above 80 percent) shortly after closure. Although not accurately represented in the models, the dryout from preclosure forced ventilation will delay by a number of years, the return to high relative humidity values at edge locations. The preclosure values of relative humidity for all scenarios should be approximately 5 percent, which is a function of the 30-percent relative humidity of the intake air for ventilation and temperature increases at the waste package. For the basecase degradation scenario, estimates of relative humidity remain low until they begin to rise at approximately 100 years. The relative humidity rises above the deliquescence lower bound in the proposed TPA Version 5.0 code beyond 200 years.

Use of the vapor pressure at boiling temperature to define the numerator for the relative humidity estimate has a theoretical ramification. The balloon analogy indicates that, as the

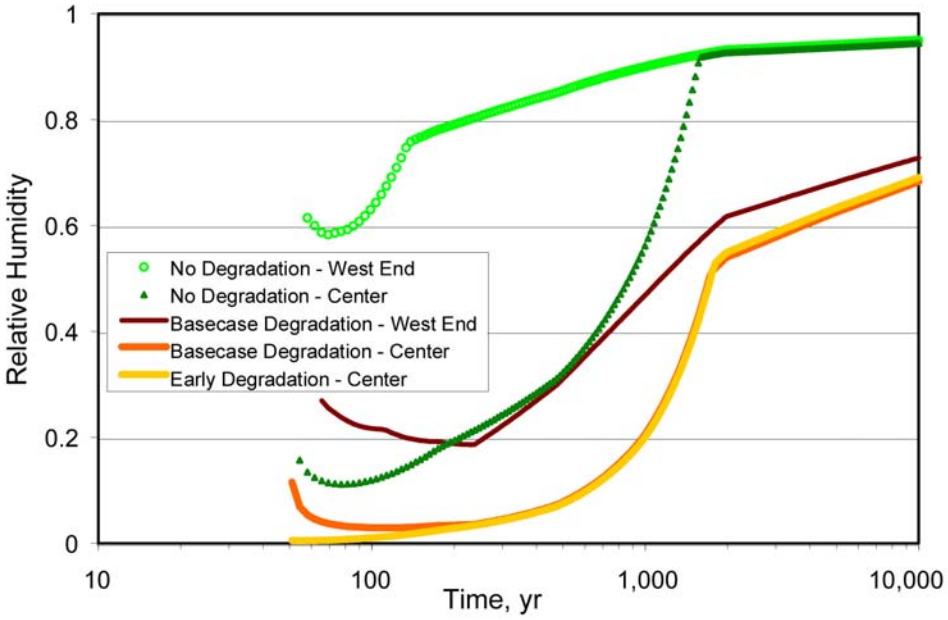

Figure 2-5. Waste Package Relative Humidity Estimates at the Center and Edge Locations of a Drift for the Basecase Degradation and No Degradation Scenarios Using Conduction-Only Model Results As the Boundary Condition for the In-Drift Heat Transfer Algorithm

boiling isotherm expands and contracts, there is no exchange of vapor across the boiling isotherm. The volume in the balloon varies, however, the pressure inside the balloon does not change. Moisture cannot enter the balloon from outside the boiling isotherm because the moisture would evaporate and return to the reflux zone, thus lowering the temperature inside the boiling isotherm. Another view is that mountain-scale circulation of gas or diurnal pressure fluctuations can induce pressure differences that lead to air exchange, particularly along the drifts. For this second view, the potential is for lower relative humidity values to occur rather than those values estimated in the balloon analogy.

2.1.3 Effect of Thermohydrology on Temperature and Relative Humidity Estimates

A linkage of the thermohydrological model and the in-drift heat transfer algorithm is used in this report to assess the abstractions used in the proposed TPA Version 5.0 code. Simulating the effects of thermohydrology on estimates of temperature and relative humidity using complex dual-permeability codes cannot directly be used for Monte Carlo simulations using the proposed TPA Version 5.0 code. The conduction-only model in conjunction with the in-drift heat transport algorithm lends itself readily to use in abstracted approaches for stochastic performance assessments. Previously, Manepally and Fedors (2003) evaluated the effect of thermohydrology on waste package temperature estimates by linking a mountain-scale conduction-only model to a detailed process model using MULTIFLO Version 1.5.2 code. The process model was a thermohydrological, dual-permeability representation of the fractured porous media that included the effect of climate change. In this report, instead of using a temperature estimate from a conduction-only model as a boundary condition, a temperature

estimate from a two-dimensional thermohydrological model is used for the boundary conditions in the in-drift heat transfer algorithm. The results are shown in Figure 2-6.

Because spatial and temporal variations in water content will affect thermal properties of the wallrock, the thermohydrological model should provide more reliable temperature estimates. The thermohydrological model is able to account for variations in percolation rates and thermal conductivity. Because the latter is a function of saturation and lithology, it varies in space and time. Both matrix and fracture continua are included in the thermohydrological model. The two-dimensional model is perpendicular to the drift and extends from the drift center to the centerpoint between drifts. The domain extends from the ground surface to the water table, and there is significant grid refinement in the vicinity of the drift. Because the model is two dimensional, it can provide results only at a specified position along a drift. To incorporate the effect of mountain-scale thermal processes, the heat load is scaled for locations based on distance from the center of a drift using results from the mountain-scale conduction-only model. A climate change model is used of modern climate for 600 years, followed by 1,400 years of monsoonal climate, then a glacial transition climate for the remainder of the performance period. More details about the thermohydrological model can be found in Manepally and Fedors (2003). Estimates of drift wall temperature from Manepally and Fedors are used as boundary conditions in the in-drift heat transfer algorithm. The in-drift heat transfer algorithm represents in-drift conduction, convection, and radiation in a more physically realistic manner than the thermohydrological model.

Figure 2-6(a) illustrates the effect of thermohydrology on waste package temperature estimates for the basecase degradation scenario, and similarly, Figure 2-6(b) for the no degradation scenario. Early in the thermal period, the effective thermal conductivity is near the saturated value. As the thermal pulse dries out the wallrock, however, the effective thermal conductivity decreases, approaching the dry thermal conductivity value when the rock is nearly completely dried out. The overprint of climate change is evident in Figure 2-6, particularly for the change to a glacial-transition climate at 2,000 years.

Relative humidity in Figure 2-7 is calculated using the temperature estimates at the waste package derived from the in-drift heat transfer algorithm that used the thermohydrological model-derived boundary conditions. Using thermohydrological results instead of conduction results for the outer boundary condition in the in-drift heat transfer algorithm leads to a shift in the profile such that a value of 50-percent relative humidity is reached 389 years sooner (488 instead of 877 years) for the no degradation scenario. The edge location remains above 50-percent relative humidity regardless of the source of input for the temperature boundary condition. Because of large differences in the wallrock and waste package temperature for the degradation scenario, there is little change in the relative humidity profile when thermohydrological results are used in the heat transfer algorithm instead of the conduction-only model results.

2.1.4 Onset and Duration of Temperature Conditions Conducive to Corrosion

The onset and duration of waste package temperature conditions in the range 80–140 °C [176–284 °F] are important for determining the potential for localized corrosion of the engineered barrier system. The upper bound for the temperature window of 140 °C [284 °F] is chosen because the corresponding maximum relative humidity would be 24.7 percent, which

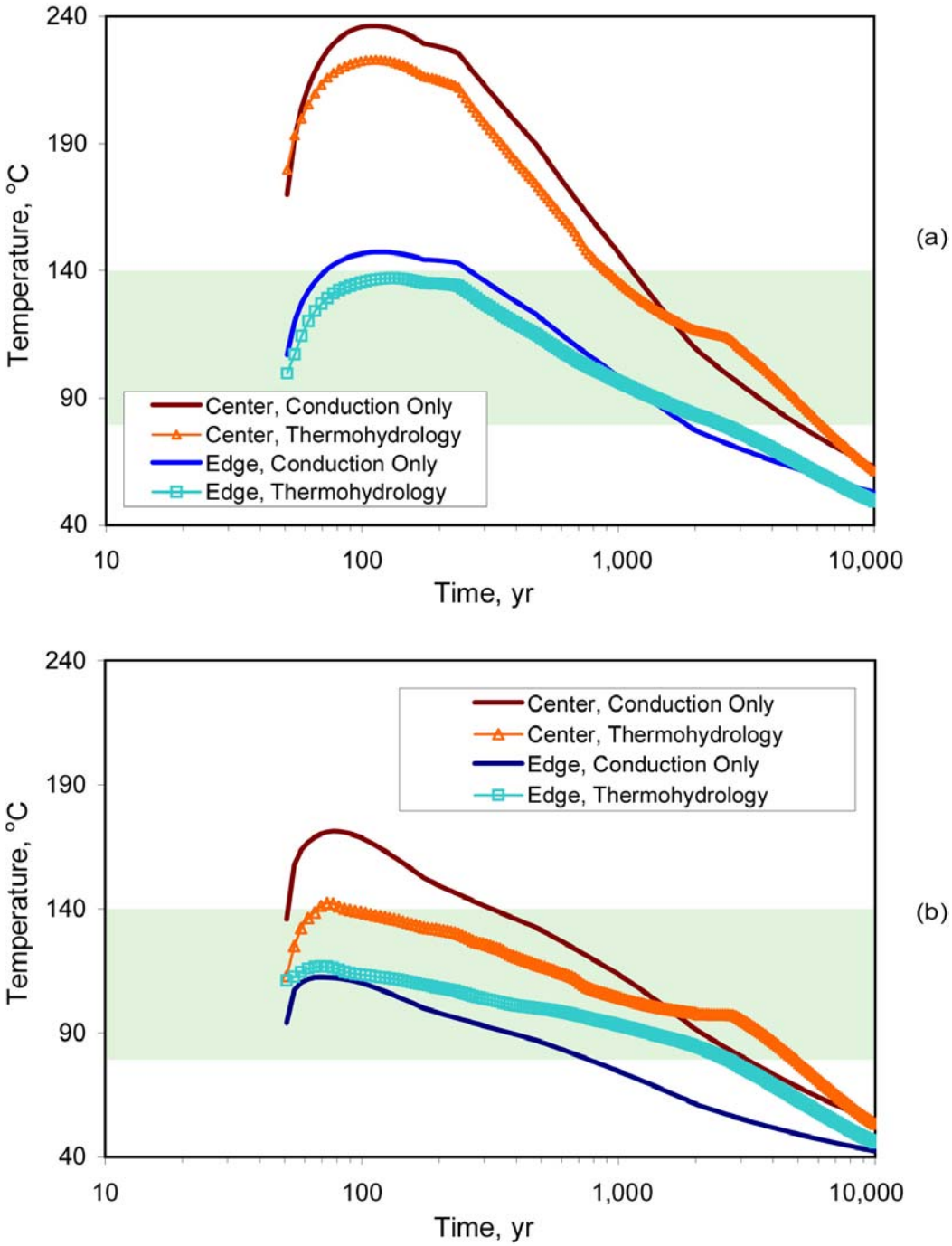

Figure 2-6. Waste Package Temperature Estimates at the Center and Edge of a Drift for the (a) Basecase Degradation and (b) No Degradation Scenarios Using Conduction-Only and Thermohydrological Model Results As the Boundary Condition for the In-Drift Heat Transfer Algorithm. Shaded Areas Mark Zone of Temperature Conditions Conducive to Corrosion [°F = (1.8 × T °C + 32)].

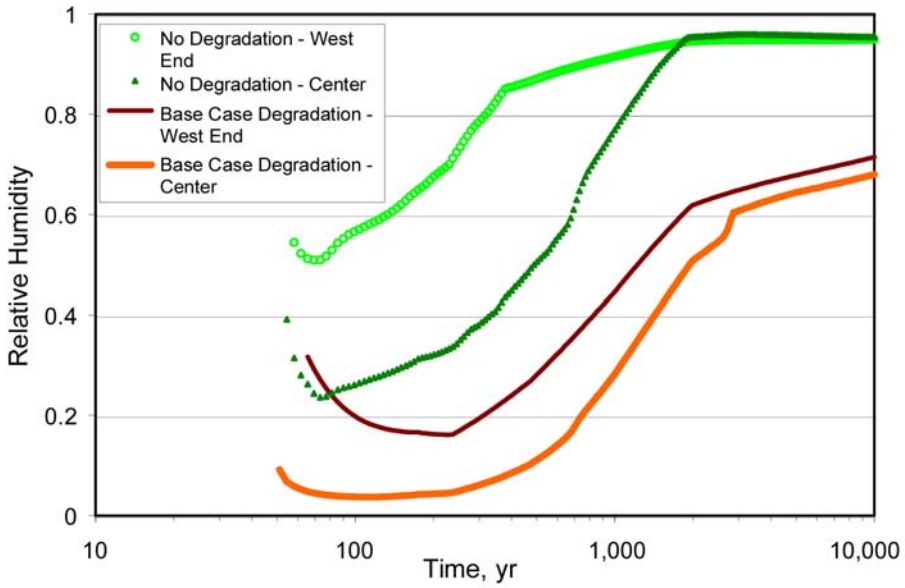

Figure 2-7. Waste Package Relative Humidity Estimates at the Center and Edge Locations of a Drift for the Basecase Degradation and No Degradation Scenarios Using Thermohydrological Model Results As the Boundary Condition for the In-Drift Heat Transfer Algorithm

is approximately the lower bound for deliquescence relative humidity used in the proposed TPA Version 5.0 code (Mohanty, et al., 2002b). The chosen lower bound of approximately 80 °C [176 °F] is based on the suggestion of Dunn, et al. (2003) and Brossia, et al. (2001) that localized corrosion of Alloy 22 is highly unlikely under anticipated repository conditions. Because the propagation rate of localized corrosion of Alloy 22 is fast once initiated, the onset time is more important than the duration. Based on parameter values used in the proposed TPA Version 5.0 code, the duration is important only if it is less than approximately 80 years.

Table 2-1 presents results for the basecase degradation and no degradation scenarios at the center and end of a typical drift in the middle of the repository. The onset and duration of conditions in Table 2-1 are relevant to the waste package environment and are based on an assumed instantaneous emplacement of all waste. The basecase degradation scenario leads to a later onset of temperature conditions conducive to corrosion of waste packages, which suggests emplaced backfill might be an advantageous strategy. Furthermore, when the effect of thermohydrology is incorporated into the heat transfer algorithm, the onset is earlier at the center locations for either scenario than when thermohydrology is not considered.

2.2 Drift-Scale Temperature Gradients in Open Drifts

To evaluate the effect of axial natural convection on temperature and relative humidity estimates, the influence of the porous media needs to be used as input to computational fluid dynamics models of in-drift air flow. Estimates of drift-scale temperature gradients derived from processes acting in the porous media are discussed in this section. Chapter 3 introduces

Table 2-1. Onset and Duration of Temperature Conditions Conducive to Localized Corrosion When the Temperature Boundary Condition for the In-Drift Heat Transfer Algorithm Is Based on the Conduction-Only or Thermohydrological Model

Scenario	Peak Temperature, °C*		Duration of Number of Years within 80 < T °C < 140		Onset Year of Temperature Window	
	Conduction Only	Thermohydrological	Conduction Only	Thermohydrological	Conduction Only	Thermohydrological
Center, No Degradation	171	142	2,751	4,722	325	86
West Edge, No Degradation	113	117	684	2,543	51	51
Center, Basecase Drift Degradation	236	223	3,814	5,403	1131	900
West Edge, Basecase Drift Degradation	146	137	1,395	2,429	232	51

*NOTE: °F = (1.8 × T °C + 32)

drift-scale modeling of natural convection using computational fluid dynamics models. Only the no degradation scenario is considered; therefore, the results are relevant for convection in open drifts.

A model that addresses the entirety of in-drift and wallrock thermohydrological processes is extremely demanding computationally, except possibly on a small scale. The approach in this section is to evaluate axial gradients using the computationally efficient conduction-only model, and then evaluate the effect on the gradients when the effect of hydrology is included through the use of a three-dimensional thermohydrological model of half a drift.

2.2.1 Gradients Based on the Conduction-Only Model

A mountain-scale conduction-only equation is used to evaluate the magnitude of repository-scale temperature gradients that reflect the edge cooling effect and the changes in lithology along a drift. Increased heat transfer at the edge of the repository leads to the edge cooling effect. The conduction-only model is used to estimate temperatures along a drift located in the middle of the repository. This is the conduction-only model that provided outer boundary condition temperatures for the in-drift heat transfer algorithm in Section 2.1. The effects of drift degradation, thermohydrology, and in-drift heat transfer are not included in the conduction-only model results presented in this section.

The selected drift for these analyses is in the center of the repository, and it is referred to as a typical drift. This analysis focuses on half of a drift because, if there are no variations in lithology, the results for one half would mirror the results of the other half. For the selected drift, the lithology varies in the eastern half of the drift but not in the western half of the drift. The two lithologic units are the Topopah Spring middle nonlithophysal unit (Tptpmn) in the east and the Topopah Spring lower lithophysal unit (Tptpll) in the center and west. Representative effective thermal conductivity values of 1.945 W/m-K [26.98 BTU/ft-h-°F] and 1.61 W/m-K [22.3 BTU/ft-h-°F] are used for the two units to estimate temperatures along the drift at the drift wall. These representative values of thermal conductivity are the average of the saturated and dry thermal conductivities for each of the lithologies.

Based on the mountain-scale conduction-only model, the drift wall temperature estimates can be used to evaluate the repository edge cooling effect by analyzing the temperature difference between the center and edge locations [Figure 2-8(a)] and the local temperature gradient [Figure 2-8(b)]. Using data only from the eastern half of the typical drift, which includes a change in lithology, Figure 2-8 illustrates the results of the two alternative perspectives on temperature gradients that could affect along-drift convective air flow.

The portion of the drift that exhibits the effect of edge cooling increases with time, although the temperature difference and the local temperature gradient decrease with time. Near lithologic changes, elevated local gradients persist beyond 2,000 years. This persistence suggests that areas near lithologic changes may be zones of elevated axial air flow and condensation.

The portions of the half drift with specific temperature differences (relative to the center location) and specific temperature gradients are plotted as a function of time in Figure 2-9(a). A similar analysis for the western half of the typical drift, which has no change in lithologic units, is presented in Figure 2-9(b).

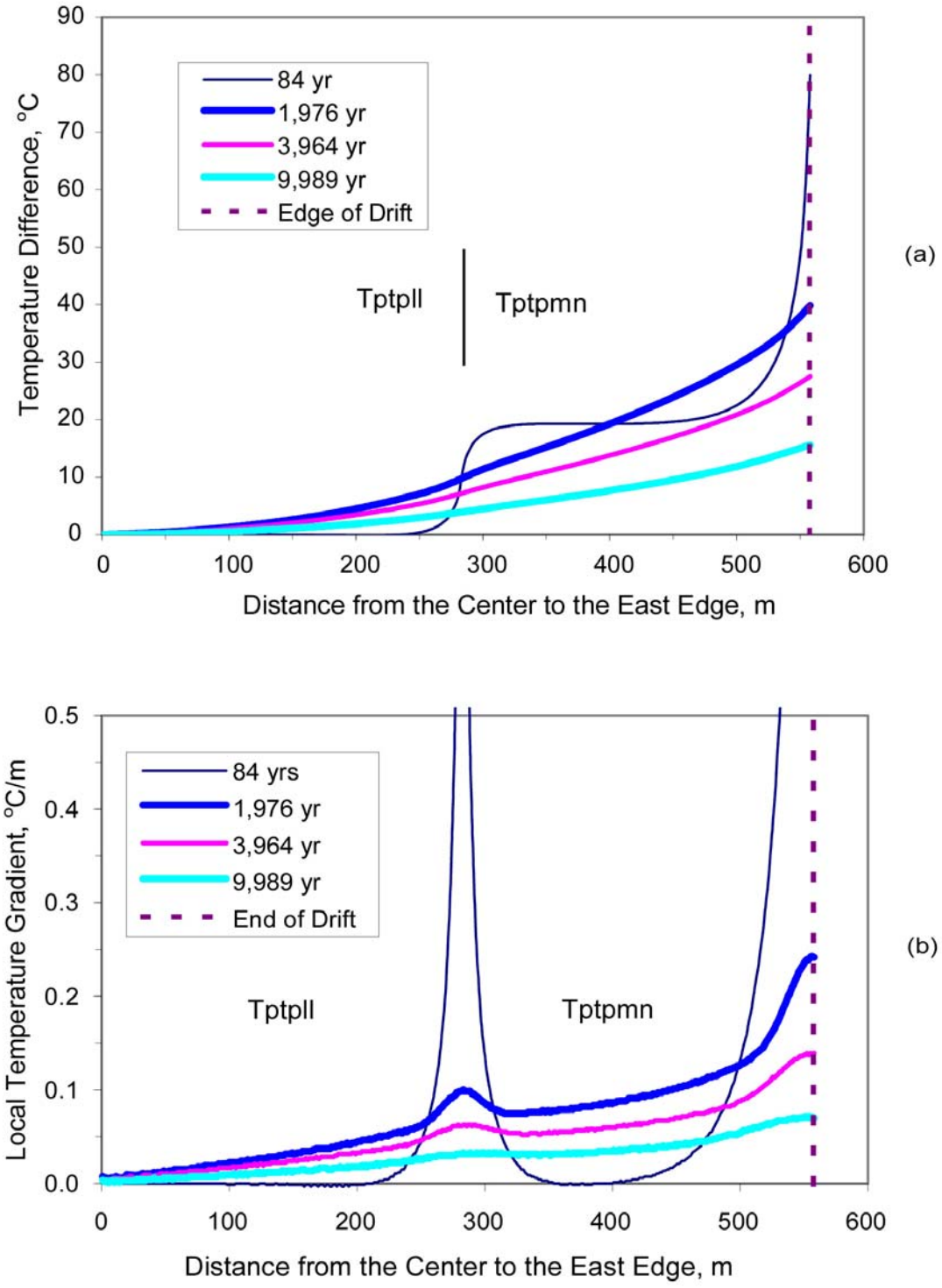

Figure 2-8. Estimated (a) Temperature Differences and (b) Local Gradients Along the Eastern Half of a Typical Drift. The Specified Times Include the 50-Year Preclosure Period [°F = (1.8 × T °C + 32); 3.3 ft = 1 m; 1.82 °F/ft = 1 °C/m].

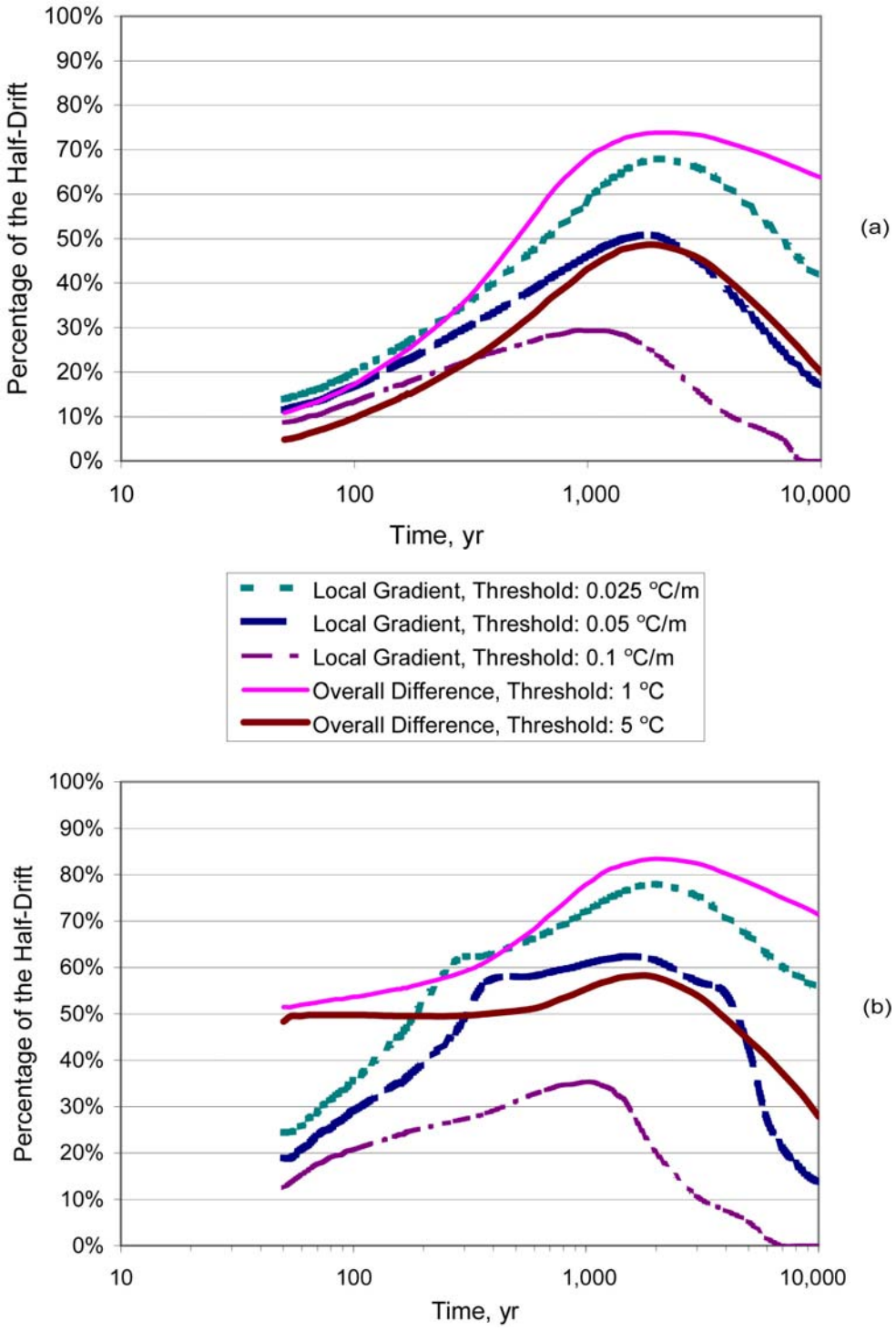

Figure 2-9. Estimated Portions of the (a) East and (b) West Halves of a Typical Drift with Temperature Differences and Local Gradients for the Specified Threshold Values [1 °F/ft = 0.55 °C/m; 1.8 °F =1 °C]

The threshold for temperature differences or temperature gradients needed to drive natural convection along a drift is not known, although the magnitude of temperature gradients should correlate with the magnitude of axial air flow rates. Thus, curves are presented for a range of thresholds for temperature differences and gradients. The magnitude of cross-sectional convection that will constrain axial convection is not known. Computational fluid dynamics modeling in Chapter 3 addresses the issue of cross-sectional air flow hindering axial convective patterns. Even using the most stringent threshold presented in Figure 2-9, approximately 30 percent of each half drift will have local temperature gradients potentially capable of driving axial convection and moisture redistribution.

2.2.2 Effect of Thermohydrology on Temperature Gradients

The mountain-scale conduction-only model does not include the effect of hydrology. Spatial and temporal variations in water content will affect the effective thermal properties of the wallrock. The required assumption for the conduction-only model is that representative values of thermal properties can be used to adequately estimate temperature profiles along a drift. Effective thermal conductivity is the most sensitive thermal property needed for the conduction-only model. Because dual-permeability models implicitly account for variations in thermal conductivity as a function of space and time, they can be used to confirm reasonableness of effective thermal conductivity estimates used in the conduction-only model. Computationally efficient two-dimensional dual-permeability thermohydrological models were developed for selected locations along a drift. Because the assumption of two-dimensional heat transfer becomes more questionable farther from the drift center, a three-dimensional thermohydrological model was developed.

Estimates from the conduction-only and thermohydrological models are expected to differ. The conduction-only model uses a constant value for thermal conductivity, whereas the thermohydrological model allows thermal conductivity as a function of saturation. Early in the thermal period, the thermal conductivity is near the saturated value. As the thermal pulse dries out the wallrock, thermal conductivity approaches the dry value. After the thermal peak passes, the zone with elevated saturation will begin to move inward, and, supported by ambient percolation, the drift walls will begin to rewet. Later, as ambient conditions return, the percolation flux from a future, glacial-transition climate leads to thermal conductivity values near the wet thermal conductivity value. Rewetting the wallrock will lead to increases in the relative humidity and the increased likelihood for liquid-phase water to occur on the drip shields and waste packages. For the Topopah Spring lower lithophysal unit, the wet and dry values for thermal conductivity used in this model are 2.02 and 1.2 W/m-K [28.0 and 16.6 BTU/ft-h-°F]. Using temperature estimates from the thermohydrological model, representative effective thermal conductivity values can be approximated for use in the conduction-only model.

The three-dimensional model of half a drift is able to incorporate lateral heat transfer, including hostrock processes of conduction, convection in gas phase, advection in liquid phase, and latent-heat transfer. Whereas the two-dimensional thermohydrological model decouples the heat transfer processes from the dimensionality, the three-dimensional model is fully coupled.

The grid for the three-dimensional model is derived from that used in the ventilation study (Painter, et al., 2001). The model inputs were updated to include the proposed TPA Version 5.0 code heat load and the active fracture implementation currently available in MULTIFLO Version 1.5.2 code. The modeled region is a slab that extends from the water table to the

ground surface, though the type of boundary conditions used at the top and bottom limit utility of the grid to early times (500–1,000 years), depending on the heat load and thermal properties. The grid includes one-half an emplacement drift, thus taking advantage of the east-west symmetry of drifts. Symmetry also is used to reduce the grid domain in the other horizontal dimension by including a region from the center of the pillar between drifts to the center of the drift opening. The grid is unstructured with grid refinement near the drift opening. There are 440 cells for each continua, matrix and fracture, in each vertical slice of the grid. Twenty vertical slices comprise 30-m [98-ft] panels along the drift. A value of 10 mm/yr [9.39 in/yr] is used for mass flow at the top boundary. At all sides of the domain, a general temperature boundary condition is used (i.e., temperature is set to a constant value at some specified distance away from the computational domain).

The objective for the three-dimensional thermohydrological simulations is to determine maximum temperature gradients along a drift to bound computational fluid dynamics modeling of axial air flow. If axial air flow is hindered by cross-sectional air flow above each waste package for most of the drift length, then assessment of the effect of the cold-trap process need only focus on short drift segments. Focusing on short drift segments will greatly reduce the computational burden of modeling natural convection and the cold-trap process. Maximum temperature gradients along a drift are expected to occur early in the performance period, hence, the thermohydrological simulations will focus on the first hundred years. At later times, temperature gradients will be decreasing, thus reducing the portions of drifts with prominent axial flow.

The conduction-only results are compared with results from the two- and three-dimensional thermohydrological models in Figure 2-10. The two-dimensional thermohydrological results,

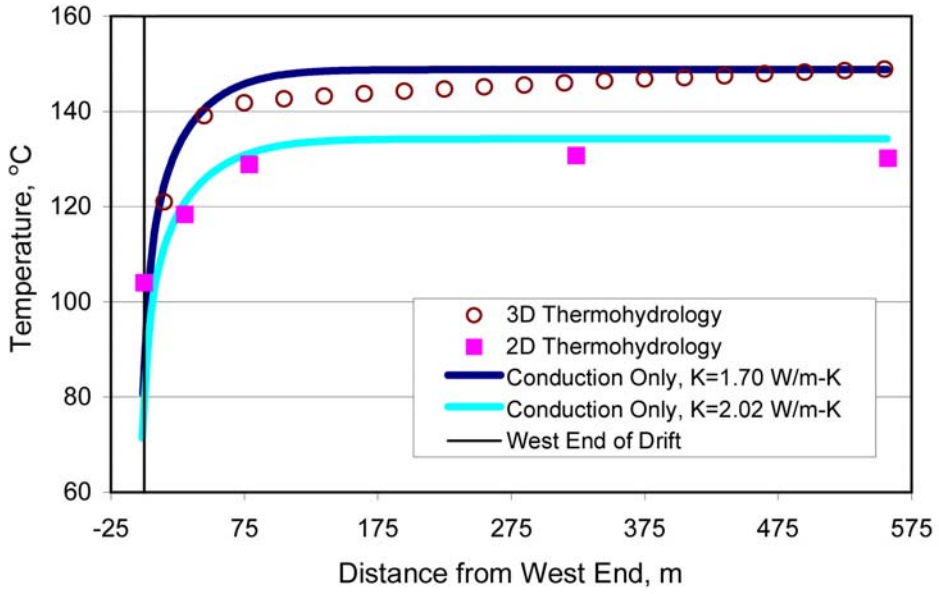

Figure 2-10. Drift-Wall Temperature Estimates from the Two-Dimensional (2D) and Three-Dimensional (3D) Thermohydrological Models Compared with Those from the Conduction-Only Model Using Two Different Values for Representative Thermal Conductivity at a Time of 109.1 Years. Vapor Phase Lowering Was Not Used [°F = (1.8 × T °C + 32); 3.3 ft = 1 m; 1 BTU/ft-h-°F = 13.9 W/m-K].

simulated at five separate locations along the drift, were extracted from Manepally and Fedors (2003). The heat load reduction factors used in the two-dimensional model results were based on conduction-only model results that used a saturated thermal conductivity value. The two-dimensional thermohydrological model results closely match the conduction-only results when the latter used a representative effective thermal conductivity value of 2.02 W/m-K [28.0 BTU/ft-h-°F], possibly reflecting a self-consistency rather than an accurate indication of the conditions. Two important differences are noted in Figure 2-10. One, the percolation rate of 6.0 mm/yr [0.24 in/yr] at early times in the two-dimensional model leads to temperatures lower than predicted by the conduction-only model. The lower temperature is likely caused by advection of heat in the liquid phase. The other difference is the two-dimensional thermohydrological results estimate higher temperatures at the extreme end of the drift. This discrepancy may be caused by the no flux (heat and mass) condition on the lateral boundary of the domain, when clearly there will be some transfer of heat and mass along the axial direction of the drift.

The results of the three-dimensional thermohydrological model also are presented in Figure 2-10 and overlie the results from the conduction-only model when a representative effective thermal conductivity value of 1.70 W/m-K [23.6 BTU/ft-h-°F] is used in the latter model. The value of 1.70 W/m-K [23.6 BTU/ft-h-°F] was selected for use in the conduction-only model to best match the spatial temperature profile from the thermohydrological model at 109.1 years. The slope of the temperature profile along the drift for the three-dimensional thermohydrological model results indicates axial heat transfer in the wallrock which may be caused by both lateral conduction (edge effect) and spatial changes in thermal conductivity because of changes in saturation along the drift. Other processes that may affect axial heat transfer include one or more of the following: (i) convection in gas phase, (ii) advection in liquid phase, and (iii) latent heat transfer. When the option in the MULTIFLO Version 1.5.2 code to include vapor phase lowering is enabled, overall temperatures along the drift are reduced (Figure 2-11). When vapor phase lowering is included, a representative effective thermal conductivity of 1.82 W/m-K [25.2 BTU/ft-h °F] is the appropriate value to use in the conduction-only model to replicate the thermohydrological effects at 109.1 years. It is not known if the difference in results between the conduction-only and thermohydrological models is important for axial natural convection. Future computational fluid dynamics modeling will be needed to assess the significance of small differences in axial gradients.

2.3 Summary

Estimates of temperature and relative humidity are needed in performance assessment analyses of a potential repository to evaluate the integrity of the engineered barrier system by assessing the chemistry of water contacting waste packages and drip shields and their potential for corrosion.

An in-drift heat transfer algorithm is used together with either a mountain-scale conduction model or a thermohydrological model to estimate temperature conditions at various locations along a typical drift. Relative humidity is estimated directly from the temperature estimates of the waste package and drift wall using simple assumptions on the moisture content of the gas phase above and below the boiling point of pure water. The onset and duration of conditions conducive to localized corrosion are estimated for the basecase degradation and no

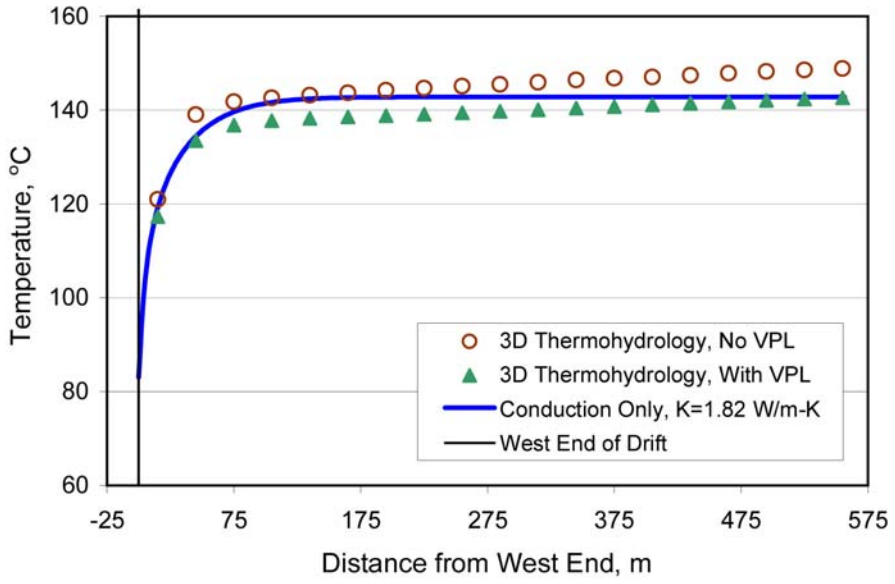

Figure 2-11. Comparison of Drift-Wall Temperature Estimates from the Three-Dimensional (3D) Thermohydrological Model with and without Vapor Phase Lowering (VPL) at 109.1 Years
[°F = (1.8 × T °C + 32); 3.3 ft = 1 m; 1 BTU/ft-h-°F = 13.9 W/m-K]

degradation scenarios. Conditions conducive to localized corrosion {80<T °C<140 [176<T °F<284]} occur much earlier at locations not in the center of drifts. Because the proposed TPA Version 5.0 code currently uses the center locations of subareas, its results may not be conservative. Compared to conduction-only model results, thermohydrology is shown to reduce the onset time and lengthen duration of the conditions conducive to localized corrosion and, therefore, should be factored into performance assessment analyses.

Next, the mountain-scale conduction-only model is used to define portions of a drift estimated to exhibit specified temperature gradients. Portions of a drift that exhibit temperature gradients vary widely with time, but appear to range from 20 to 65 percent during the times of interest for potential localized corrosion of Alloy 22. The uncertainty in the range is directly tied to the uncertainty in the threshold to use for temperature gradients. These estimates of the portion of a drift that exhibit the specified temperature gradient, however, do not include the effect of hydrology. Results from a three-dimensional model simulation using MULTIFLO Version 1.5.2 are provided as a comparison to the estimates of temperature from the conduction-only model. The three-dimensional thermohydrological model accounts for the spatial and temporal variations in effective thermal conductivity. The thermohydrological results indicate a temperature gradient exists along the drift because of the variation in effective thermal conductivity and saturation; this gradient does not occur when using the conduction-only model. It is not known, however, what magnitude of temperature gradient would be important for axial convection and moisture redistribution. Thus, temperature variations along a drift also are developed to support computational fluid dynamics modeling of in-drift air flow and moisture redistribution.

Natural convection will affect temperature profiles along drifts and modify local temperature variations across the engineered barrier system. Estimates of temperature and relative humidity presented in this section did not incorporate these effects. Chapter 3 specifically addresses issues related to natural convection and describes ongoing efforts to develop simulation tools and laboratory data needed to validate those tools.

3 MODELING NATURAL CONVECTION IN HEATED DRIFTS

Natural convection and the cold-trap process will modify in-drift temperature and moisture distributions along emplacement drifts at the potential high-level waste repository at Yucca Mountain, Nevada. Temperature and relative humidity are important inputs for assessing chemistry of water contacting engineered barrier components and potential corrosion of those components. The U.S. Department of Energy (DOE) has not provided a basis to exclude these processes, nor have these processes been adequately included in models supporting documented performance assessments. DOE approximates the effect of radial heat transfer in their two-dimensional thermohydrological models, but does not include moisture redistribution or the heterogeneity of three-dimensional heat transfer in the complex geometry of emplacement drifts. In addition, axial natural convection and moisture redistribution are expected to occur (Bechtel SAIC Company, LLC, 2003a), but no analyses have been provided by DOE. In preparation for reviewing future DOE analyses, U.S. Nuclear Regulatory Commission (NRC) and Center for Nuclear Waste Regulatory Analyses (CNWRA) have undertaken laboratory and numerical modeling investigations to explore and identify importance issues associated with natural convection and the cold-trap process on temperature and moisture estimates along drifts.

Computational fluid dynamics modeling is an important tool for understanding in-drift air flow patterns and rates because of their ability to incorporate the buoyant effects of thermally perturbed air. Computational fluid dynamics modeling can be used to help understand the extent and magnitude of axial convection and moisture redistribution along drifts. In addition, assessing small-scale spatial variations of temperature around the engineered components (e.g., waste packages and drip shields) requires computational fluid dynamics modeling of air flow. Natural convection around the engineered barriers may be important for assessing the nonuniformity of temperature and relative humidity around waste packages and the drip shield and for assessing the potential dispersion of acidic gases formed from evaporation of concentrated water. These local zones within the complex geometry of the engineered barrier system are not addressed in this report, but will be addressed in future studies.

Air flow patterns between eccentrically located cylinders, geometrically similar to the waste package and drift wall, were extensively studied by Kuehn and Goldstein (1978). Their investigations provide support for computational fluid dynamics simulations of small length scales. Francis, et al. (2003) simulated the Kuehn and Goldstein data as part of a validation exercise prior to using computational fluid dynamics models to estimate effective thermal conductivity values for air that reflect convective heat transfer. Francis, et al. (2003) used measured data from the DOE 25- and 44-percent-scaled convection tests at the Atlas Facility and assumed the estimated properties would also be applicable to the emplacement drifts. It is important to note that heat transfer coefficients had to be calibrated for the scaled laboratory experiments because of difficulties in matching temperatures surrounding the analog waste packages using standard heat transfer models at interfaces of solid material and air. Although Francis, et al. (2003) did not attempt to evaluate axial air flow or moisture redistribution, their work does provide a glimpse into the possible approach DOE will take in addressing Agreements TEF.2.04 and TEF.2.05 on the cold-trap process. Danko and Bahrami (2004) attempted to simulate axial convection and condensation using a compartmentalized in-drift air flow model linked to a porous media model for the wallrock. They estimated that significant portions of drifts would exhibit axial air flow and high condensation rates, however, measured data to support their model inputs appear to be lacking. Possible measured data to support

axial convection and moisture redistribution in emplacements are limited to small-scale experiments or ventilated tunnels. Air flow in small-scale experiments is generally laminar, whereas air flow in the emplacement drifts is expected to be turbulent. Thus, little support for the highly uncertain heat transfer coefficients at the interface of solid materials and air can be provided by the small scale experiments. Because forced ventilation models require the use of mixed convection models for heat transfer at the interfaces of solid materials and air, they similarly do not appear to be applicable to the enclosed potential emplacement drifts at Yucca Mountain during the postclosure period. Simulations of the Climax Test (Patrick, 1986) illustrate the difficulty in adequately matching measured data for a ventilated experiment. Adequacy of models for heat transfer from solid surfaces to the air was identified as a reason heat removed by the ventilation was not adequately matched. Measured data in support of axial flow patterns and magnitudes and moisture redistribution through evaporation, gas phase transport, and condensation may be provided by the Passive Test at Yucca Mountain (Bechtel SAIC Company, LLC, 2003c). It is not clear, however, if sufficient quantitative or qualitative observations in the Passive Test were made prior to elimination of the thermal gradient induced by periodic operation of the tunnel boring machine. It is also not clear if seepage can be delineated from condensation, or if any spatial information was collected when the thermal gradient was present.

Individually, natural convection, thermal radiation, conduction, and latent heat-transfer processes are reasonably well understood, however, the combined effects of all heat-transfer processes in geometrically complex environments are poorly understood and difficult to model. Axial drift convection and latent-heat transfer attempt to dampen axial temperature gradients. Offsetting dampening is the effect of heat flux out the drift and thermal radiation, which serves to sharpen the temperature gradient between hot and cold locations. The intimate linkage of in-drift natural convection and condensation to heat and mass transfer in the host rock complicates modeling efforts because both porous media and computational fluid dynamics codes may be necessary. The need to understand the combined effect of fundamental processes involved in the movement of moisture driven by convection necessitated developing laboratory, analytical, and numerical models.

Preliminary drift-scale computational fluid dynamics models are presented in Section 3.1. These models are used to assess two potentially important aspects of natural convection in the heated drifts that, if shown to be unimportant, would simplify the modeling effort.

- Are variations in fluid (air and air plus water vapor) properties expected to significantly influence modeling results?

- At what temperature gradients do cross-sectional flow patterns limit axial convection cells?

In Section 3.2, simulation results are presented for a laboratory experiment using a porous ceramic cylinder surrounded by variably saturated sand to represent a drift located in fractured rock. A temperature gradient inside the drift was induced by placing a heater cartridge at one end of the cylinder and a heat sink at the other end. The variably saturated sand was intended as a source of water for inside the cylinder. This benchtop laboratory experiment has been completed and the final computational fluid dynamics simulation results are presented in this section. Previously, these simulations did not include the effect of phase change and latent-heat transfer (Walter, et al., 2004; Fedors, et al., 2003b). This section also presents

preliminary information on two other ongoing laboratory experiments. One experiment is designed to help understand moisture movement and condensation in a tightly controlled environment. The other experiment more closely matches the geometry of the emplacement drift, but at a 20-percent scale.

3.1 Drift-Scale Simulation with Single Component Gas

Simulation of the flow and heat transfer processes in a full-scale repository drift loaded with waste packages entails large-scale natural convection flow, water phase change at the walls, and thermal conduction in the walls. Temperatures along the drift are estimated to vary widely throughout the life of the repository; so, the gas in the drift can be a highly variable composition of air and water vapor. Before including the effects of evaporation and condensation on the flow field, it is beneficial to investigate the effects of a single component gas in the drift without the complications of the phase change process at the walls.

The first objective of this analysis is to compare the estimated flow velocities and temperature profiles of a repository drift in which the gas is either dry air or pure water vapor. This investigation will reveal the sensitivity of the fluid dynamics and the thermal response of the repository to water vapor concentration.

The second objective is to determine if the gas circulation and temperature vary significantly over a long section of drift. This investigation will reveal whether a full three-dimensional flow simulation is required or the drift can be simulated as independent two-dimensional flow fields in the cross section of the drift.

3.1.1 Drift-Scale Model Description

A 200-m [656-ft] length of drift from a closed end was simulated with FLOW–3D® using a three-dimensional mesh. The drift diameter is 5.5 m [18.0 ft], and a nonporous invert was modeled in the bottom of the drift. Waste packages are individually simulated in the outer 60 m [197 ft] of the drift segment. A line load is used instead of individual heat sources for the inner portion of the drift segment. Waste packages were simulated using 1.8-m [5.9-ft] diameter by 5.1-m [16.7-ft] long cylinders. The waste packages were placed at 6.1-m [20.0-ft] intervals. To determine if axial natural convection can be excluded from future analyses of the cold-trap process, temperature gradients at early times in the performance period are used in simulations. Temperature gradients are expected to be greatest during the first 100 years. The waste package power output specified was 2,150 W [7,338 BTU/h] per waste package, which is appropriate for the time of 109.1 years using the proposed TPA Version 5.0 code (Mohanty, et al., 2002b) parameters. A mesh spacing of 0.29 m [0.95 ft] was used near the closed end of the drift, and the mesh spacing expanded to nearly 3.9 m [12.8 ft] at the opposite end of the drift. A mesh-independence study was not performed, so results should be considered preliminary. The use of a no-flow boundary at the end of the hot end of the mesh is consistent with the attainment of a constant temperature (no edge effect) at this internal position of the drift.

A 1-m [3.3-ft] thick rock layer surrounding the drift was included in the simulation. The temperature at the outer surface of this rock layer was specified consistent with estimates from a conduction-only model using parameters from the basecase proposed TPA Version 5.0 code for 109.1 years. Early in the postclosure period, temperature gradients near the edge of the

repository are greater than at later times. Thus, conditions at 109.1 years may be considered a bounding case for along-drift temperature gradients that drive axial convection. The rock surface temperature 1 m [3.3 ft] outside the closed end of the drift is specified as 80 °C [176 °F] and increases in a nonlinear fashion to 127 °C [261 °F] at a location 200 m [656 ft] from the closed end. The rock surface temperature is assumed to be circumferentially uniform at each axial location.

3.1.2 Drift-Scale Simulation Results

The simulations were run until the overall fluid kinetic energy and thermodynamic energy were varying less than 1 percent, indicating a nearly steady-state condition. The three-dimensional simulation results were processed to provide cross-sectional average values for the gas temperature and volumetric flow rate as a function of distance from the closed end.

The gas circulation rate is computed by integrating the fluid velocity of the cross section for all locations where the gas is moving away from the closed end of the drift. A closed boundary was assumed for these simulations; therefore, at any given cross section along the drift axis, the flow of gas away from the closed end of the drift is balanced by flow toward the closed end. Because a closed boundary is used, the effects of barometric pumping or natural convection through the surrounding fractured tuff cannot be simulated using this model. So, the gas circulation rate is the volumetric flow of gas exchanged between volumes on either side of a plane at the specified axial location.

The calculated gas circulation rates for dry air and pure water vapor are compared in Figure 3-1. There are some slight differences between the two sets of results, however, the gas circulation rates for the two gas compositions are in close agreement. The circulation rate is strongest at the closed end of the drift where the gas circulates between the hot waste package and the relatively cooler end wall. The circulation rate decreases with the distance from the hot end of the drift segment. There is a sharp decrease in axial flow rate over the first 120 m [394 ft] of the

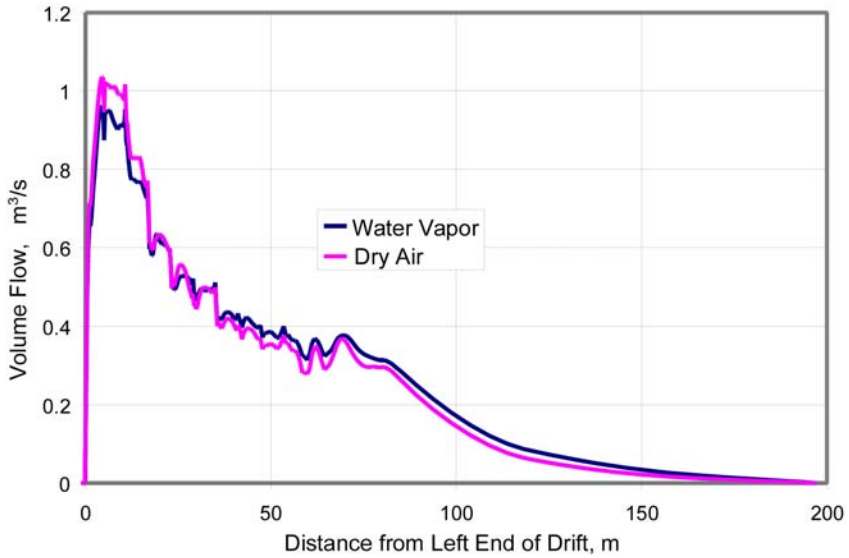

Figure 3-1. Estimated Axial Circulation (Gas Phase) Rate [3.3 ft = 1 m; 35.3 ft^3/s = 1 m^3/s]

drift segment and a smaller decrease asymptotically to zero for the remaining 75 m [246 ft]. The axial fluid temperature profile is shown in Figure 3-2. Similar to the gas circulation rates, this graph shows the average temperature in the drift cross section is virtually identical for both dry air and pure water vapor. The cross-sectional mean temperature varies by only 5 °C [9 °F] along the drift, while the rock temperature increases approximately 47 °C [85 °F] along the drift. This temperature information indicates the circulation tends to mix the gas and decrease the effects of the axial variation in rock temperature.

There are axial variations not present from 60 to 200 m [197 to 656 ft] in the circulation rate and fluid temperature for locations less than 60 m [197 ft] from the closed end. These variations are indicative of the mesh expanding in the axial direction away from the closed end. The coarser mesh cannot resolve the geometric details around waste packages greater than 60 m [197 ft] from the closed end. The computational fluid dynamics model in these locations is essentially for a 140-m- [459-ft]-long cylinder with a heat generation rate per unit length consistent with locations closer than 60 m [197 ft] from the closed end.

Two conclusions may be drawn from these computational fluid dynamics results. First, it is clear the temperature and circulation rates for pure air and water vapor are approximately equal. This equality implies details of the gas composition do not strongly affect the overall simulation of fluid dynamics and heat transfer in the drift. The overall temperature and overall gas flow rates do not depend on the precise composition. Therefore, properties of the gas phase do not have to account for the variations in vapor mole fraction in future modeling efforts. The second conclusion is cross-sectional air flow patterns do not eliminate axial convection for conditions representing a time of 109.1 years in emplacement drifts. As noted earlier, temperature gradients are largest near the ends of drifts at early times. Temperature gradients from distances of 100 to 150 m [328 to 492 ft] are approximately 0.01 °C/m [0.005 °F/ft]. Thus, the conditions at 109.1 years represent a bounding case for evaluating the effect of cross-sectional

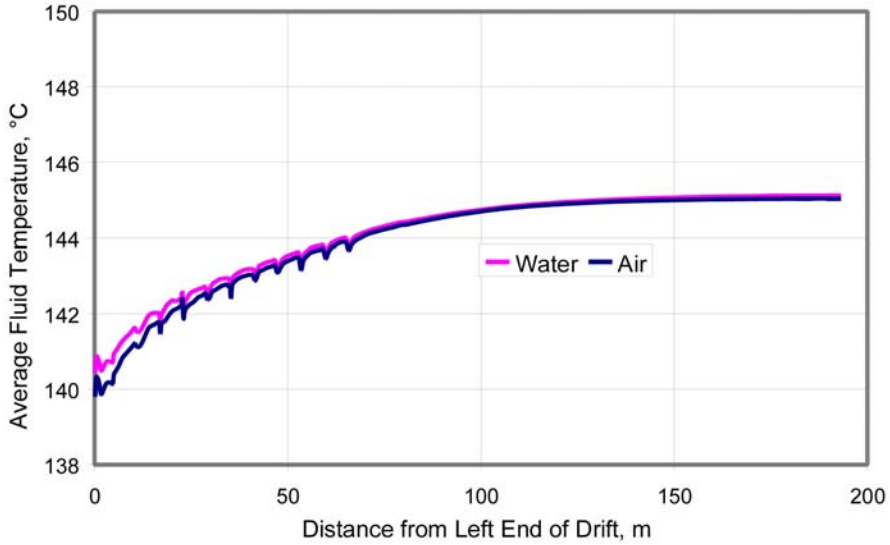

Figure 3-2. Estimated Axial Fluid (Gas Phase) Temperature Profile [3.3 ft = 1 m; °F = (1.8 × T °C + 32)]

air flow patterns on axial air flow. The axial flow decreases slightly more strongly than linearly but is significant enough far away from the drift end to modulate the axial gas temperature variation.

3.2 Benchtop Experiment Simulation Results

A small, prototype laboratory-scale experiment was designed, assembled, and conducted to investigate vapor driven air movement and condensate formation induced by the cold-trap effect in a simulated emplacement drift. This 1:100 scale experiment (Figure 3-3) was modeled using a computational fluid dynamics code, FLOW–3D®, in an attempt to further understand the experimental results and to develop numerical modeling techniques that could be used to model larger scale experiments and the full-scale Yucca Mountain waste package emplacement drift. A description of the experiment and FLOW–3D® model inputs and mesh can be found in Walter, et al. (2004) and Fedors, et al. (2003b). This prototype laboratory experiment was useful for identifying numerical model features and property measurement needs to support a larger scale experiment and drift-scale modeling.

The initial modeling effort did not match the experimental results with a high level of accuracy (Fedors, et al., 2003b). One reason identified for the poor match between the model and the experiment was the lack of a phase change model in the computational fluid dynamics code. A phase change model was developed and implemented into FLOW–3D® that accounts for the mass transfer and latent heat transfer associated with the evaporation and condensation of water in the drift (Green, et al., 2004). The laboratory experiment was remodeled using this new model. A comparison of the phase change model results with the previous nonphase change model results is summarized in this section.

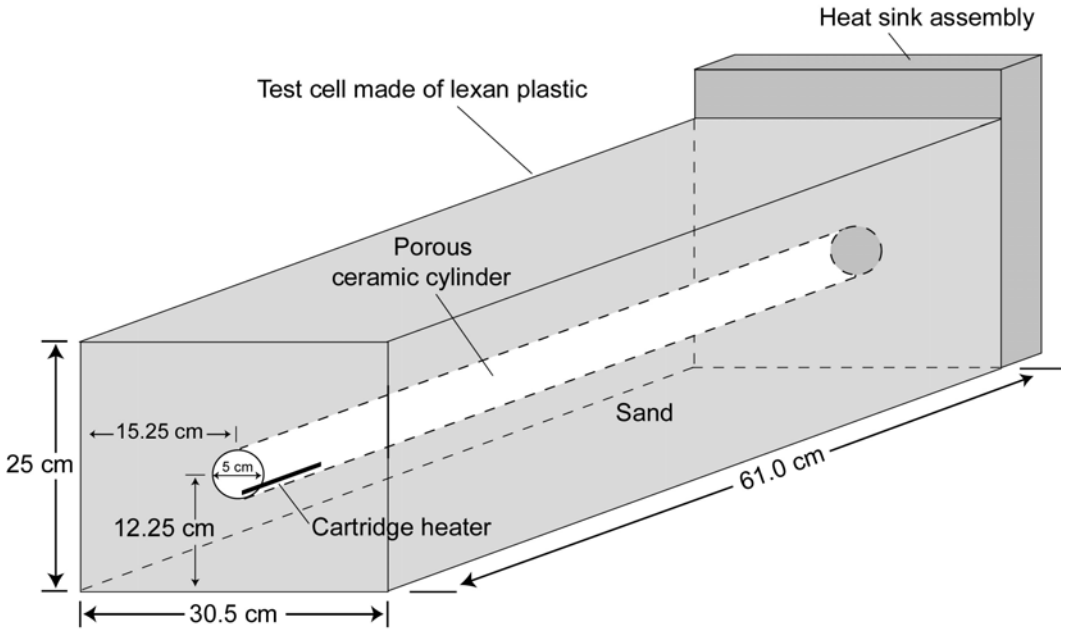

Figure 3-3. Schematic Drawing of Benchtop Cold-Trap Experiment [1 in = 2.54 cm]

The comparison between the two models is made by analyzing the gradient of the average fluid temperature, the total air flow rate, and the net vapor flow rate along the drift. Figure 3-4 shows a comparison of the average fluid temperatures estimated by the two models. These temperature data were generated by calculating the area weighted average fluid temperature at each cross section along the drift axis.

The results show the phase change model had little effect on the temperatures except near the heater. The phase change model lowered the fluid temperatures in the region near the heater. The average temperature throughout the rest of the drift is nearly the same for the two models. Even in the heater region, the phase change model results are only approximately 1 °C [1.8 °F] lower than the nonphase change model results. These results suggest that neglecting latent heat transfer in the benchtop experiment was not responsible for the difficulty in matching temperatures in the air above the heater. Because latent heat transfer does not appear to be significant for the benchtop experiment, the difficulty in matching measured data should focus on unknown power leakages or the heat transfer models at interfaces of solid material and air near the heat source. Difficulties in matching measured data at the DOE Atlas Facility natural convection tests (Bechtel SAIC Company, LLC, 2003a) and the mixed (forced) convection conditions at the Climax Test (Patrick, 1986) similarly pointed towards heat transfer models at interfaces of solid material and the air.

Figure 3-5 shows a plot of the total fluid flow rate and the net vapor transport rate for the two different models. The postprocessing methodology for the total air flow rate is identical for the nonphase and phase change model results. The total air flow is nearly identical for the two models except for the region near the heater, where the nonphase change results are slightly

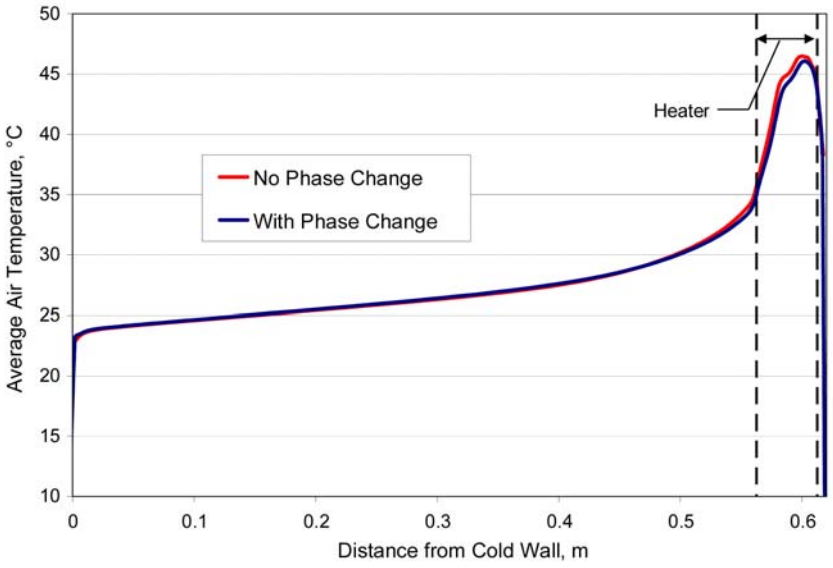

Figure 3-4. Average Fluid Temperatures Estimated Using FLOW–3D®, with and without Phase Change [3.3 ft = 1 m; °F = (1.8 × T °C + 32)]

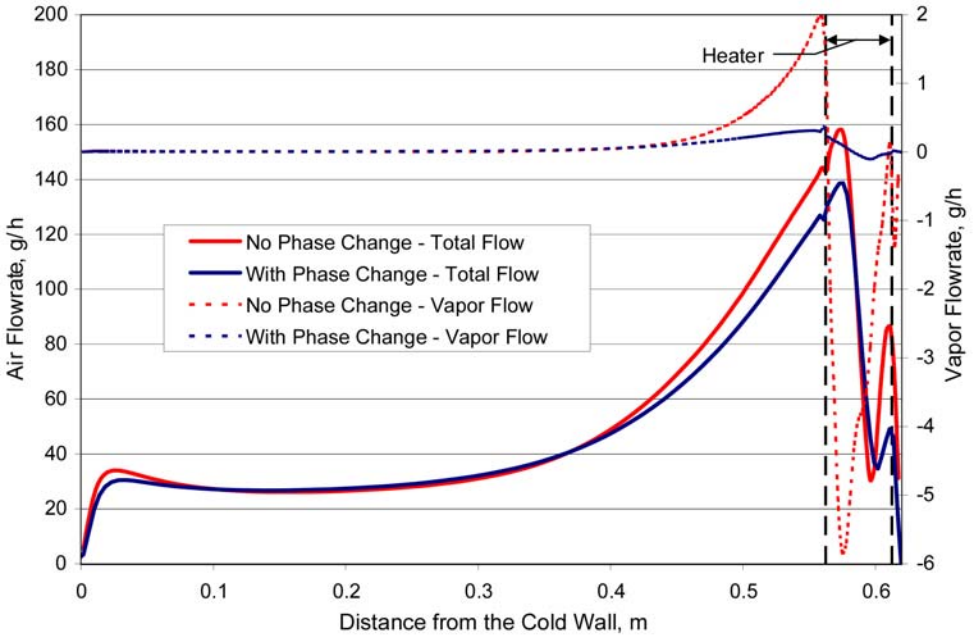

Figure 3-5. Estimated Bulk Air and Vapor Flow Rates Using FLOW–3D®, with and without Phase Change [3.3 ft = 1 m; 1 lb/h = 454 g/h]

higher than the results from the model with phase change. The fluid flow rate is calculated by summing the product of the axial velocity, area, and density for all cells in each drift cross section. Because the simulations use an incompressible fluid model, the net air fluid flow at each cross section is zero. The fluid flow rates shown in Figure 3-5 refer only to the component of flow moving from the cold wall end toward the heater.

The postprocessing calculations for the net vapor flow rate are unique for the two different models. For the model with nonphase change, the net vapor flow rate is simply the sum of the product of the mass flow rate and the vapor concentration for all cells in each drift cross section. For the nonphase change model, the vapor transport must be inferred from the dry air results. Assumptions are made that all air in the drift is at saturated conditions and that latent heat, because of evaporation and condensation, is negligible compared with the overall heat transfer rate. With these assumptions, the vapor transport is determined by calculating the saturated vapor concentration of each cell based on the cell fluid temperature. This concentration is then used to calculate the net vapor flow rate in an identical manner to that used for the phase change model results. Because the vapor flow rate is presented as a net value, it describes the difference in transport rates at a particular drift cross section of the moisture traveling toward and away from the heater.

The total axial flow rate in the plane at the end of the heater is approximately 10 percent less for the case when phase change is included in the calculations. Variations in the cross sections containing the heater are greater than those away from the heater. At a position 0.4 m [1.3 ft] from the cold end, however, the total axial flow velocity results are virtually identical for the two models. The net vapor flow rate results show a more significant variation between the two models than the total flow rate. The axial vapor flow rate in the plane at the end of the heater

for the phase change case is approximately 15 percent of the case when vapor flow is inferred from the air-only calculations. In the heater region, the variation in the two sets of results is even more pronounced. The discrepancy is mainly because the assumption regarding completely saturated fluid is not valid, especially near the heater. These results show there is much less vapor transport than if a fully saturated assumption is made.

Figure 3-6 further explains this conclusion by showing a contour plot of the relative humidity near the heater (results are from the model with phase change). The plot shows the air entering the heater region from the cold wall end (lower left hand region) is greater than or equal to 100-percent relative humidity. Supersaturated air is allowed in the model for fluid away from solid surfaces. Supersaturated air in regions far from solid surfaces should be viewed as fog; that is, condensation on particles in the air may occur, which may remain suspended in the air. As the heater raises the temperature of the air, the vapor diffusion rate is not adequate to keep the air saturated, thereby causing the humidity to drop. As the air travels back toward the cold wall, it cools because of natural convection and picks up moisture through diffusion and evaporation at the drift wall. Because of this prominent nonsaturated region near the heater shown in Figure 3-6, 100-percent relative humidity used in a simplified model by Fedors, et al., (2003b) is not a valid assumption for the nonphase change model.

It is important to note these results and conclusions are based solely on computational fluid dynamics modeling. In this study, no attempt was made to make comparisons with the experimental results because of the difficulty in matching the measured results described by Fedors, et al. (2003b) possibly due to inadequacy of the heat transfer model at solid-air interfaces. The small size (1-percent scale) of the benchtop experiment logistically precluded precise measurements later deemed important for computational fluid dynamics modeling. This prototype laboratory experiment, however, did provide valuable insights to guide the study of convection and the cold-trap process in heated drifts and the development of large-scale experiments that are more appropriate for emplacement drifts.

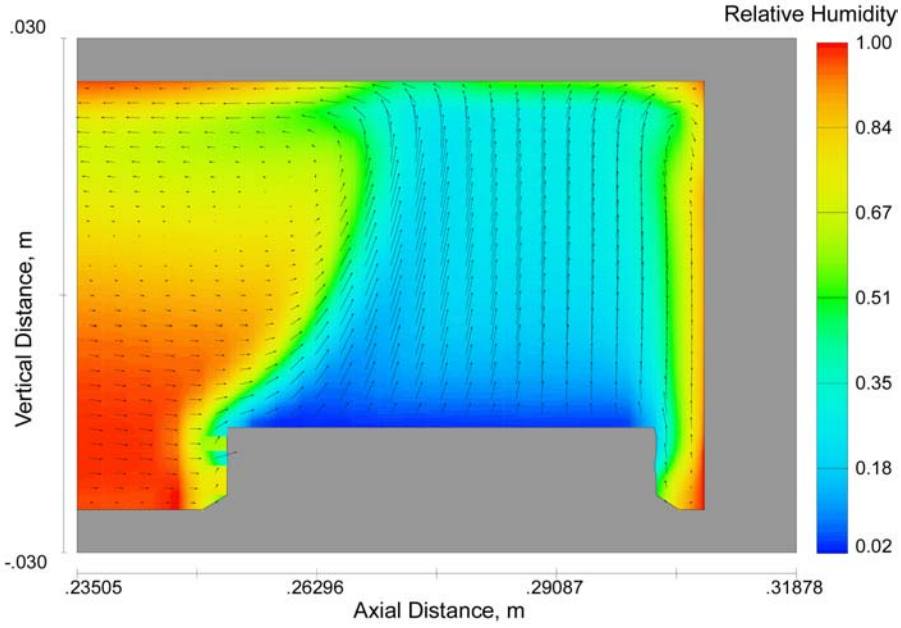

Figure 3-6. Relative Humidity Contour Plot in the Region near the Heater Estimated Using FLOW–3D® with Phase Change [3.3 ft = 1 m]

These computational fluid dynamics results are adequate to draw two conclusions that will be helpful in future computational fluid dynamics modeling efforts. One conclusion, at least for this scale experiment, is the phase change model has little effect on the temperature and a moderate effect on the overall fluid flow. The other conclusion is that latent heat transfer does not appear to be responsible for difficulties in matching measured temperatures near the heat source. To better match the measured data, calibrating the computational fluid dynamics model to heat transfer coefficients at the interfaces of solids and air near the heat source may be required; this unfortunately renders the model less useful in predictive mode, particularly when scales and geometries significantly change.

3.3 Ongoing Laboratory Experiments

Besides the benchtop experiment described in Section 3.2, two other laboratory experiments are ongoing. These two experiments will provide measured data to support the parameters used in the computational fluid dynamics models. The first experiment is a small condensation cell that intends to provide data for moisture redistribution using a geometry that allows tight control of conditions, although not necessarily a geometry analogous to the emplacement drifts. The second experiment is an approximate 20-percent scale model of the emplacement drift with up to four analog waste packages providing a heat source in a long pipe. The valuable insights learned from the prototype benchtop experiment guided many of the design features of the 20-percent scale experiment. These two ongoing experiments are briefly described next.

3.3.1 Condensation Cell

Laboratory tests with tightly controlled conditions are designed to validate the water transport models added to the FLOW–3D® computational fluid dynamics code. The code modules were added (with the assistance of Flow Science, Inc.) to simulate water evaporation at a heat source, water condensation on cool surfaces, and the associated latent heat transfer. Tests are being conducted to measure water evaporation and water condensation rates in a natural convection flow. Comparisons will be made between the measured water transport rates and the rates calculated by the computational fluid dynamics model. Tests are being conducted to measure the amount of water transported from the water source to the condensation plate. Four tests will be conducted: three tests will be conducted by varying the heat rate to the water source and measuring the steady-state temperatures and water transport rate and a fourth test with no water.

Pretest computational fluid dynamics model simulations were used to determine the dimensions of the condensation cell to (i) ensure conditions in the cell were amenable to two-dimensional modeling, (ii) determine size of free water surface and power needed to heat that water, (iii) determine the size and operating temperature of the cold plate, (iv) define the operating conditions for testing, and (v) make sure the moisture transport rate would be high enough to be easily measured.

A schematic and photographs of the test rig are shown in Figure 3-7. The enclosure is made of polycarbonate sheet (clear) and aluminum. The cell is 53-cm long, 15-cm tall, and 30-cm deep [23-in long, 6-in tall, and 12-in deep]. Water is condensed and collected on the aluminum plate shown on the left side of the test enclosure. Water evaporates from the pan shown on the bottom-left of the enclosure. Instrumentation has been included to measure the evaporator

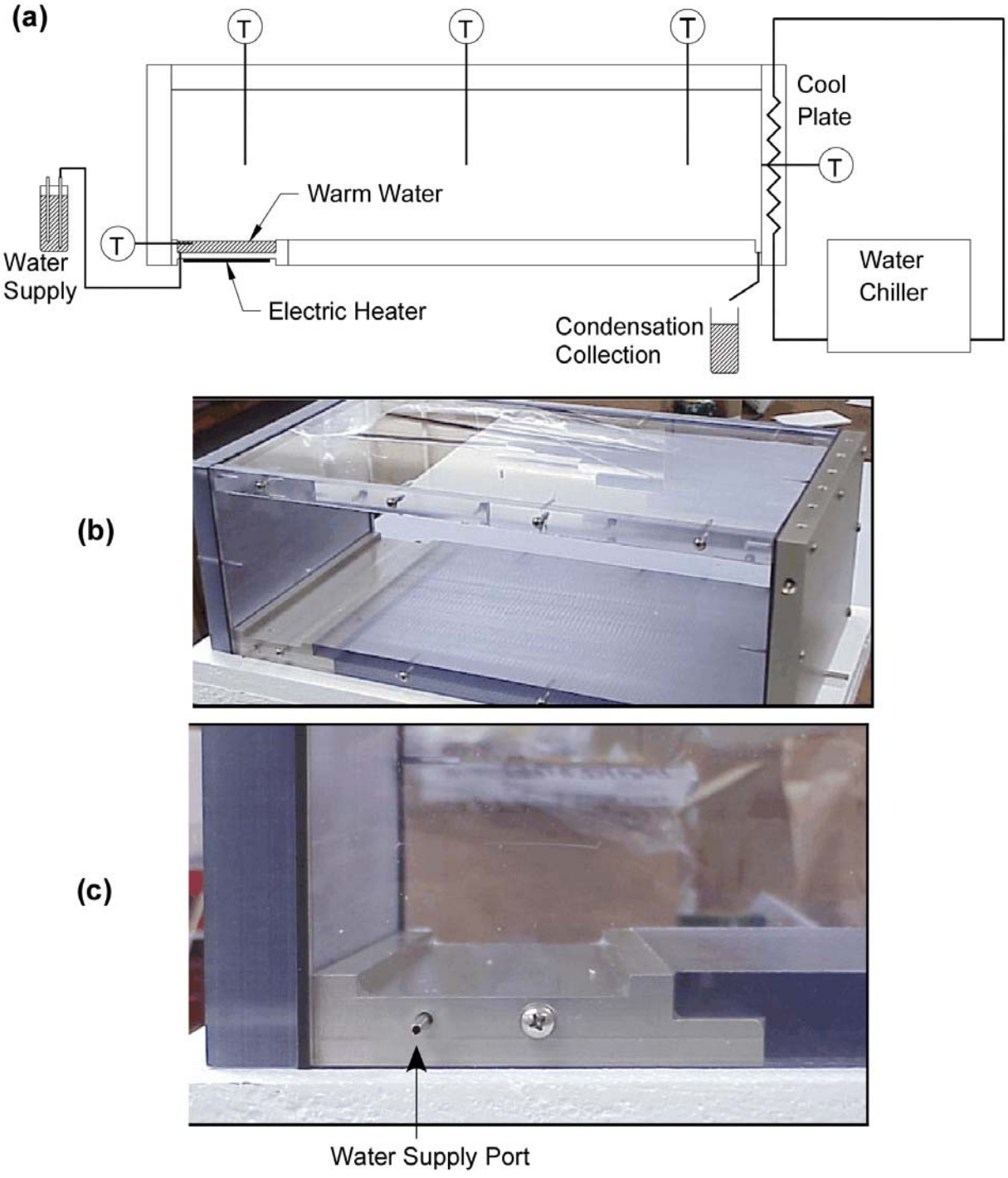

Figure 3-7. (a) Design Schematic of the Condensation Cell. Photographs of (b) Condensation Cell and (c) Water Supply Port and Depression Inside Cell [T = Thermocouple for Measuring Temperature]

(water) temperature, condenser temperature, air temperatures, water evaporation rate, and the water condensation rate.

3.3.2 The 20-Percent Scale Experiment of a Drift

This section describes a larger-scale laboratory experiment being developed to evaluate processes governing temperature and moisture redistribution in a heated enclosed tube scaled to approximately 20 percent of a proposed emplacement drift at Yucca Mountain. This experiment does not replicate expected in-drift conditions at Yucca Mountain, but rather aims to (i) develop a fundamental understanding of the cold-trap process and (ii) effectively represent the cold-trap process in numerical models used to simulate in-drift conditions during the postclosure period. Currently, an open-drift design has been implemented to simplify the range of processes occurring in the experiment. As testing proceeds, additional features such as a drip shield and natural backfill can be added.

To overcome the difficulties associated with upscaling results from small bench-top experiments to the drift scale at Yucca Mountain, an experiment designed at 20-percent drift scale was developed. Details of this experiment are provided in the following section.

3.3.2.1 The 20-Percent Drift-Scale Design

The 20-percent drift-scale experiment is being constructed and tested. The 20-percent drift-scale experiment was proposed as a means to gain additional insights into the cold-trap process that were not possible with the 1-percent bench-scale prototype laboratory experiment. Based on estimates of Rayleigh numbers from Fedors, et al. (2003b), air flow in the benchtop experiment remained in the laminar range using approximate ranges for eccentric cylinders as reported in Kuehn and Goldstein (1978). The Rayleigh number describes the relative magnitude of buoyancy and viscous forces in the fluid (air). Length scale dramatically changes estimates of Rayleigh numbers, thus it is expected that air flow in the 20-percent scale experiment and the emplacement drifts will be turbulent. In addition to its size, the new experiment incorporated four 20-percent scaled waste packages that were heated to simulate postclosure conditions. The inclusion of four waste packages supports simulating the effects of uniform and nonuniform heat loads on the evolution of the cold-trap process.

Temperature and relative humidity distributions will be measured during the heating phase of the experiment to provide insights into the cold-trap process. Although direct measurements of air flow would provide important information in support of natural convection and the cold-trap process, accuracy is low for devices available to measure air flows at the expected low velocities. For this reason, direct measurements of air flow are not currently planned. Qualitative observations, such as the release of colored gases, have been tested and appear to provide useful information on circulation patterns and turbulence.

The experiment uses a polyvinylchloride pipe closed on each end to simulate the enclosed environment [Figure 3-8(a)]. Because the physical and chemical properties of the pipe differ significantly from the walls of the potential repository at Yucca Mountain, it is obvious the experiment will not serve as an exact analog for Yucca Mountain. The choice of the polyvinylchloride pipe was, in part, governed by the need to reduce complex boundary interactions (e.g., vapor and air diffusion across boundaries and water sorption along bounding walls) that would occur with other materials such as concrete, thereby reducing complex

(a)

(b)

(c)

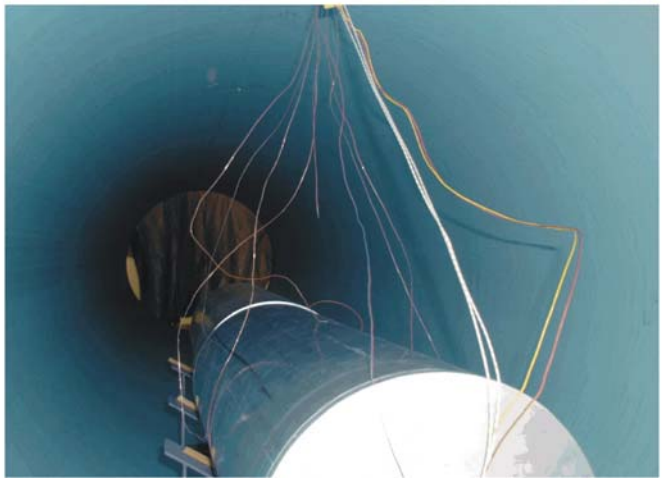

Figure 3-8. Photographs of the 20-Percent Drift-Scale Natural Convection and Cold-Trap Laboratory Experiment with (a) Polyvinylchloride Pipe, (b) Four Analog Waste Packages and Stands, and (c) Waste Packages Inside the Pipe with Thermocouples for Preliminary Testing

interactions that could complicate understanding the fundamental processes governing the cold-trap process. The internal diameter of the pipe is approximately 1.056 m [41.8 in], the external diameter is approximately 1.125 m [44.3 in], and the length is approximately 6.096 m [20 ft]. The end caps of the pipe are made of 6.4-cm- [0.25-in]-thick low thermal conductivity Lexan® to minimize heat loss.

The analog waste package is similarly scaled to approximately 20 percent of the proposed waste package dimensions for Yucca Mountain. Four aluminum analog waste packages were constructed. Each waste package is approximately 30.5 cm [12 in] in diameter and approximately 0.998 m [39.3 in] in length. Extending internally from one face of each waste package is a heating rod. The rod will be heated in the presence of a vacuum {5 in Hg [17 kPa]} inside the analog waste package so that its walls are heated by radiation. Figure 3-8(b) shows the fabricated analog waste packages. The current design has the waste packages aligned end-to-end, but not touching, and resting on stands.

3.3.2.2 System Monitoring

Temperature and relative humidity will be actively monitored during the experiment. Temperature monitoring will be performed using a series of nested calibrated thermocouples along the surfaces of the waste packages suspended in the air, and along the inner and outer walls of the pipe. The latter combination will support estimation of the heat flux across the pipe boundary. Relative humidity is monitored using a series of sensors placed at specified locations. Locations of the nested thermocouples and relative humidity sensors are based on the computational fluid dynamics simulations performed to date. Figure 3-8c shows some of the thermocouples installed in the pipe. Maintaining a vacuum in the analog waste packages ensures that radiation is the dominant process inside the waste package, thus leading to application of a uniform heat load. The vacuum is monitored before and after each test phase.

3.4 Summary

Natural convection is expected to modify temperature gradients along drifts and within the complex engineered barrier system, and to enhance evaporation, moisture transport, and condensation above that expected by diffusion alone. An evaluation of the magnitude of temperature and moisture redistribution in drifts caused by natural convection, however, has not been provided by DOE. Documentation is scheduled for release summer 2004. To explore and identify specific areas of uncertainty, CNWRA initiated laboratory and numerical investigations of natural convection and the cold-trap process in drifts. Besides preparing to evaluate future DOE analyses, these investigations can provide a bases for incorporating the effects of natural convection and cold-trap process in NRC performance assessment simulations. This chapter reported on the progress of CNWRA computational fluid dynamic simulations of in-drift conditions and supporting laboratory experiments.

A three-dimensional drift-scale model of a 200-m [656-ft] drift segment was developed. For temperature gradients along drifts relevant for a time of 109.1 years, drift-scale computational fluid dynamics modeling concluded that axial air flow will occur in spite of strong cross-sectional air flow patterns. Because it was shown to be significant during early times in the performance period when maximum temperature gradients are expected to occur, axial flow cannot be excluded from natural convection investigations. At early times, these temperature gradients coincide with zones where conditions are conducive to localized corrosion of Allow 22.

Although this conclusion indicates further modeling is needed to assess the effects of axial convection and the cold-trap process, it also indicates two-dimensional cross-sectional models should not be used unless a new approach is developed to account for the three-dimensional effects. The three-dimensional computational fluid dynamics simulations also suggest axial convection will occur along a line of uniformly heated waste packages when temperature gradients are as low as 0.01 °C/m [0.005 °F/ft]. Furthermore, simulations demonstrated the variation in gas phase properties as a result of variations in moisture content need not be considered in future computational fluid dynamics modeling efforts.

Measured data found in the scientific literature were found to be of marginal utility to support models of air flow and moisture redistribution in nonventilated heated tunnels. Thus, a prototype benchtop laboratory experiment was developed as previously described (Fedors, et al., 2003b). The benchtop experiment is a 1-percent scale model of the proposed drifts for Yucca Mountain. In the previous modeling effort, the computational fluid dynamics simulations of the benchtop experiment did not include latent-heat transfer. A module that includes evaporation, condensation, and latent-heat transfer was linked to FLOW–3D® as described in Green, et al. (2004). Simulations with and without the moisture module illustrate the difference in vapor flow between the approaches. Results obtained using the moisture module better represent the expected relative humidity near the heat source. The low values of relative humidity near the heat source invalidate the assumption used prior to implementation of the moisture module. Difficulties in matching measured temperatures near the heat source in the benchtop cold-trap experiment may point towards the inadequacy of standard heat transfer models at interfaces of solids and air.

Two ongoing laboratory experiments are expected to provide measured data to support computational fluid dynamics modeling of natural convection and the cold-trap process. The first experiment is a tightly controlled condensation cell designed to validate the moisture module added to FLOW–3D®. The second ongoing laboratory experiment is a 20-percent scale model of a drift segment with four geometrically scaled waste packages. This second experiment is designed to provide data relevant to the geometry of the emplacement drifts. Drift degradation was not included in the design of the 20-percent experiment to simplify the experiment, although flow blockage above a drip shield may be an added feature for additional test phases. Both experiments are in the testing and data collection phases. As a result, no data are presented in this report.

4 CONCLUSIONS

Temperature and moisture levels in the drift environment can have a significant effect on waste package integrity at the potential high-level waste repository at Yucca Mountain, Nevada. In their evaluation of the U.S. Department of Energy (DOE) approaches for estimating waste package and drift wall temperatures, the U.S. Nuclear Regulatory Commission and Center for Nuclear Waste Regulatory Analyses have identified drift degradation, repository edge cooling, and natural convection for closer examination. DOE does not include the presence of a rubble pile caused by drift degradation in their estimate of temperatures. Previous DOE thermohydrological models (CRWMS M&O, 2001a) may not have adequately represented repository edge cooling, primarily because none of the two-dimensional thermohydrological models were sited on the repository edge. DOE has not decided yet how natural convection and the cold-trap process will be addressed in a potential license application. The options are to include the effects of convection and the cold-trap process in performance assessment analyses or to provide a basis for excluding these processes. DOE analyses for repository edge cooling and cold-trap processes are scheduled for completion summer 2004.

Environmental conditions along a typical drift were estimated using an in-drift heat transfer algorithm with either a mountain-scale conduction model or a thermohydrological model to determine the temperature boundary condition in the wallrock. The onset of conditions conducive to localized corrosion of Alloy 22 for the basecase degradation and no degradation scenarios occurs much earlier at locations not in the center of drifts. Because the proposed TPA Version 5.0 code currently uses the center locations of subareas, the onset of conditions conducive to corrosion of Alloy 22 is underestimated by hundreds of years. Also, compared to conduction-only, thermohydrology is shown to reduce the onset time of conditions conducive to localized corrosion and, therefore, should be factored into the performance assessment analyses.

The computationally efficient mountain-scale conduction-only model was used to define portions of a drift estimated to exhibit specified temperature gradients. Portions of drifts exhibiting specified temperature gradients exceed 30 percent. The magnitude of temperature gradients important for driving natural convection, however, is highly uncertain. Sensitivity analyses for different magnitudes of temperature gradients were provided to illustrate the effect on estimates of the portions of a drift. Preliminary drift-scale computational fluid dynamics modeling of convection suggests temperature gradients producing axial air flow approach the lowest values used in the sensitivity analyses. In calculating temperature gradients along drifts, the conduction-only model does not include the effect of hydrology. Thus, results from a three-dimensional simulation using MULTIFLO Version 1.5.2 are provided as a comparison. The thermohydrological results indicate a temperature gradient exists along the drift because of the variation in effective thermal conductivity and saturation; this gradient does not occur when using the conduction-only model. Temperature variations along a drift were also developed to support computational fluid dynamics modeling of in-drift air flow and moisture redistribution. Temperature gradients along drifts for the early and basecase degradation scenarios were not calculated, however, these gradients may be inferred from temperature differences between the potential repository center and edge locations. During the temperature range of interest for localized corrosion, the temperature differences along degraded drifts are only slightly greater than those in open drifts. Heterogeneity of drift degradation, however, has the capability of significantly modifying axial temperature gradients and, thus, will be the focus of a future studies.

Modeling natural convection and the cold-trap processes in thermally perturbed drifts requires using computational fluid dynamics codes and measured data for validation of said models. Preliminary results of drift-scale modeling indicate axial convection in drifts will be present in spite of strong cross-sectional flow patterns. Furthermore, parameter inputs for the properties of the gas phase need not consider the variation in moisture content across and along the drifts. Although the first conclusion indicates three-dimensional computational modeling (rather than two-dimensional cross-sectional modeling) is required, the second conclusion would greatly simplify the modeling effort. Two ongoing laboratory experiments, a condensation cell and a 20-percent scale model, are expected to provide data to support the assessment of natural convection and the cold-trap process. Drift degradation will not be incorporated into the computational fluid dynamics simulations until the simpler case of an open drift can be adequately simulated.

5 REFERENCES

American Society of Heating, Refrigeration, and Air Conditioning Engineers, Inc. *ASHRAE Handbook and Product Directory, 1977 Fundamentals.* 3rd Printing. New York City, New York: American Society of Heating, Refrigeration, and Air Conditioning Engineers, Inc. 1977.

Bechtel SAIC Company, LLC. "Technical Basis Document No. 5: In-Drift Chemical Environment." Rev. 1. Las Vegas, Nevada: Bechtel SAIC Company, LLC. 2003a.

———. "In-Drift Natural Convection and Condensation Model Report." MDL–EBS–MD–000001. Rev. 00A, Draft. Las Vegas, Nevada: Bechtel SAIC Company, LLC. 2003b.

———. "In Situ Field Testing of Processes." ANL–NBS–HS–000005. Rev. 02. Las Vegas, Nevada: Bechtel SAIC Company, LLC. 2003c.

———. "Technical Basis Document No. 3: Water Seeping Into Drifts." Rev. 2. Las Vegas, Nevada: Bechtel SAIC Company, LLC. 2003d.

———. "Technical Basis Document No. 5: Waste Package and Drip Shield Corrosion." Rev. 1. Las Vegas, Nevada: Bechtel SAIC Company, LLC. 2003e.

———. "Drift Degradation Analysis." ANL–EBS–MD–000027. Rev. 02. Las Vegas, Nevada: Bechtel SAIC Company, LLC. 2003f.

———. "Risk Information to Support Prioritization of Performance Assessment Models." TDR–WIS–PA–000009. Rev. 01 ICN 01. Bechtel SAIC Company, LLC. 2002.

———. "FY01 Supplemental Science and Performance Analyses." Vol. 1: Scientific Bases and Analyses. TDR–MGR–MD–000007. Rev. 00 ICN 01. Las Vegas, Nevada: Bechtel SAIC Company, LLC. 2001.

Brossia, C.S., L. Browning, D.S. Dunn, O.C. Moghissi, O. Pensado, and L. Yang. "Effect of Environment on the Corrosion of Waste Package and Drip Shield Materials." CNWRA 2001-003. San Antonio, Texas: CNWRA. 2001.

Carslaw, H.S. and J.C. Jaeger. *Conduction of Heat in Solids*. Oxford, United Kingdom: Oxford University Press. 1959.

Claesson, J. and T. Probert. "Temperature Field Due to Time-Dependent Heat Sources in a Large Rectangular Grid-Derivation of Analytical Solution." SKB96–12. Stockholm, Sweden: Swedish Nuclear Fuel and Waste Management Company. 1996.

CRWMS M&O. "Multiscale Thermohydrologic Model." ANL–EBS–MD–000049. Rev. 00 ICN 02. Las Vegas, Nevada: CRWMS M&O. 2001a.

———. "Water Distribution and Removal Model." ANL–EBS–MD–000032. Rev. 01. Las Vegas, Nevada: CRWMS M&O. 2001b.

Danko, G. and G. Bahrami. "Coupled Multi-Scale Thermohydrologic-Ventilation Modeling with MULTIFLUX." Proceedings of the Society for Mining, Metallurgy, and Exploration Annual Meeting, February 23–25, 2004. Published on CD ROM. Denver, Colorado: Society for Mining, Metallurgy, and Exploration. 2004.

DOE. DOE/RW–0539–1, "Yucca Mountain Science and Engineering Report." Rev. 1. Las Vegas, Nevada: DOE, Office of Civilian Radioactive Waste Management. 2002.

Dunn D.S., L. Yang, Y-M. Pan, and G.A. Cragnolino. "Localized Corrosion Susceptibility of Alloy 22." 2003 Corrosion Conference, San Diego, California, March 16–20, 2003. Paper No. 03697. Houston, Texas: NACE International. pp. 1–14. 2003.

Fedors, R.W., G.R. Adams, C. Manepally, and S.T. Green. "Thermal Conductivity, Edge Cooling, and Drift Degradation—Abstracted Model Sensitivity Analyses for Yucca Mountain." San Antonio, Texas: CNWRA. 2003a.

Fedors, R.W., D.B. Walter, F.T. Dodge, S.T. Green, J.D. Prikryl, and S.J. Svedeman. "Laboratory and Numerical Modeling of the Cold-Trap Process." San Antonio, Texas: CNWRA. 2003b.

Francis, N.D., S.W. Webb, M.T. Itamura, and D.L. James. "CFD Modeling of Natural Convection Heat Transfer and Fluid Flow in Yucca Mountain Project (YMP) Enclosures." SAND2002–4179. Albuquerque, New Mexico: Sandia National Laboratories. 2003.

Green, S.T., D.B. Walter, R.W. Fedors, and F.T. Dodge. "A Model for Moisture Transport in a High-level Radioactive Waste Repository Drift." Proceedings of the Society for Mining, Metallurgy, and Exploration Annual Meeting, February 23–35, 2004. Published on CD ROM. Denver, Colorado: Society for Mining, Metallurgy, and Exploration. 2004.

Gute, G.D., G. Ofoegbu, F. Thomassy, S. Hsiung, G. Adams, A. Ghosh, B. Dasgupta, A. Chowdhury, and S. Mohanty. "MECHFAIL: A Total-system Performance Assessment Code Module for Evaluating Engineered Barrier Performance Under Mechanical Loading Conditions." CNWRA 2003-06. San Antonio, Texas: CNWRA. 2003.

Houseworth, J.E., S. Finsterle, and G.S. Bodvarsson. "Flow and Transport in the Drift Shadow in a Dual-Continuum Model." *Journal of Contaminant Hydrology.* Vols. 62 and 63. pp. 133–156. 2003

Kuehn, T.H. and R.J. Goldstein. "An Experimental Study of Natural Convection Heat Transfer in Concentric and Eccentric Horizontal Cylindrical Annuli." *Journal of Heat Transfer.* Vol. 100. pp. 635–640. 1978.

Manepally, C. and R.W. Fedors. "Edge-Cooling Effect on the Potential Thermohydrologic Conditions at Yucca Mountain." Proceedings of the 10th International High-Level Waste Management Conference, Las Vegas, Nevada, March 30–April 3, 2003. Published on CD ROM. La Grange Park, Illinois: American Nuclear Society. 2003.

Manepally, C., R. Fedors, G. Adams, and S. Green. "Effects of Drift Degradation on Environmental Conditions in Drifts." Fall Meeting Supplement, American Geophysical Union 2003 Fall Meeting, San Francisco, California, December 8–12, 2003. Eos Transactions, American Geophysical Union. Vol. 84, No. 46. 2003.

Mohanty, S., R. Codell, J.M. Menchaca, R. Janetzke, M. Smith, P. LaPlante, M. Rahimi, and A. Lozano. "System-Level Performance Assessment of the Proposed Repository at Yucca Mountain Using the TPA Version 4.1 Code." CNWRA 2002-05. Rev. 1. San Antonio, Texas: CNWRA. 2002a.

Mohanty, S., T.J. McCartin, and D.W. Esh. "Total-system Performance Assessment (TPA) Version 4.0 Code: Module Descriptions and User's Guide." San Antonio, Texas: CNWRA. 2002b.

NRC. "Risk Insights Baseline Report." Washington, DC: NRC. 2004. <http://www.nrc.gov/waste/hlw-disposal/reg-initiatives/resolve-key-tech-issues.html>

Pabalan, R.T., L. Yang, and L.B. Browning. "Effects of Salt Formation on the Chemical Environment of Drip Shields and Waste Packages at the Proposed Nuclear Waste Repository at Yucca Mountain." CNWRA 2002-03. San Antonio, Texas: CNWRA. 2002.

Painter, S., C. Manepally, and D. Hughson. "Evaluation of U.S. Department of Energy Thermohydrologic Data and Modeling Status Report." San Antonio, Texas: CNWRA. 2001.

Patrick, W.C. "Spent Fuel Test—Climax: An Evaluation of the Technical Feasibility of Geologic Storage of Spent Nuclear Fuel in Granite." UCRL–53702. Livermore, California: Lawrence Livermore National Laboratory. 1986.

Reamer, C.W. "U.S. Nuclear Regulatory Commission/U.S. Department of Energy Technical Exchange and Management Meeting on Thermal Effects on Flow (January 8–9, 2001)." Letter (January 26) to S. Brocoum, DOE. Washington, DC: NRC. 2001. <www.nrc.gov/waste/hlw-disposal/public-involvement/mtg-archive.html#KTI>

Walter, D.B., S.T. Green, R.W. Fedors, and R.A. Hart. "Modeling a Small Laboratory Cold-Trap Experiment." Proceedings of the Society for Mining, Metallurgy, and Exploration Annual Meeting, February 23–35, 2004. Published on CD ROM. Denver, Colorado: Society for Mining, Metallurgy, and Exploration. 2004.

Wilder, D.G. "Near-Field and Altered Zone Environment Report." UCRL–LR–124998. Livermore, California: Lawrence Livermore National Laboratory. 1996.

APPENDIX

IN-DRIFT HEAT TRANSFER ABSTRACTION

Heat transfer equations for the thermal network representing cases in the proposed Total-System Performance Assessment Version 5.0 abstraction are presented here for completeness. Only the backfill case was presented in Chapter 2 (Fedors, et al., 2004). The three modes of heat transfer of conduction, convection, and thermal radiation are considered for the three cases:

(1) Preclosure when no drip shield nor backfill is present
(2) Postclosure with waste package, invert, and drip shield
(3) Postclosure with waste package, invert, drip shield, and backfill with or without air space above the backfill

Three assumptions are made for the thermal network analysis. First, the assumption is made that axial temperature variation or heat flux is negligible. Second, the translation of the two-dimensional geometric configuration in a cross section of the drift to a radially oriented configuration centered on the drift centerline also is assumed acceptable. Sensitivity analyses presented by Manepally, et al. (2003) suggest the radial assumption is reasonable. Third, the outer boundary condition positioned at the drift wall is assumed adequate. Approaches for assessing the effects of the lat two assumptions are presented at the end of this appendix.

Expressions for heat load (Q_p) as a function of effective thermal conductances (G) and the temperature difference between the waste package (T_p) and the drift wall (T_w) are developed from thermal networks used to describe each case. Waste-package surface temperature is calculated after the effective thermal conductance terms have been evaluated and the drift-wall temperature has been specified. The effective thermal conductance is defined as the inverse of the resistance R, in Fedors, et al., 2004, Figure 2-1) using the electrical network analog. This thermal network approach follows that presented in Incropera and DeWitt (2002) and Mohanty, et al. (2002). Fedors, et al. (2003) noted errors in the radiation component and the conceptualization of the thermal network paths for cases 2 and 3 in Mohanty, et al. (2002) that lead to significant errors in waste package surface temperatures when the drift degradation effect was incorporated into the algorithm. Thus, modified expressions from Fedors, et al. (2003) are presented here and used in the analysis presented in the main text of Fedors, et al., (2004).

The multimode thermal network for preclosure (case 1) has radiation and convection laterally and upward through the air and conduction through the floor all acting in parallel, thus leading to the following equation for the heat load

$$Q_p = \left[\frac{1}{R_k} + \frac{1}{R_{cpw}} + \frac{1}{R_{rpw}}\right]\left(T_p - T_w\right) = \left[G_{inv} + G_{cpw} + G_{rpw}\right]\left(T_p - T_w\right) \quad (1)$$

where the resistance and effective conductance terms are defined to represent

R_k — conduction through the floor
R_{cpw} — convection between waste package and drift wall
R_{rpw} — radiation between waste package and drift wall
G_{inv} — conduction through the invert (floor)

G_{cpd} — convection between waste package and drift wall
G_{rpd} — radiation between waste package and drift wall

Because conduction through the floor, convection, and radiation operate in parallel, they can simply be added.

For postclosure cases, where a drip shield is in place, thermal processes act in series above the waste package. The drip shield blocks direct convection and radiation between the waste package and drift wall. The high thermal conductivity of the drip shield and small thickness lead to a much smaller thermal resistance than for other components of heat transfer. Thus, the drip shield can be neglected from the thermal network for heat transfer, but its effect on separating the regions above and below the drip shield for radiative and convective heat transfer must still be included. The multimode thermal networks for postclosure in lead to the following equations for no backfill (case 2)

$$Q_p = \left[G_{inv} + \left(\frac{1}{G_{cpd} + G_{rpd}} + \frac{1}{G_{cdw} + G_{rdw}} \right)^{-1} \right] \left(T_p - T_w \right) \tag{2}$$

where the effective conductance terms are defined to represent

G_{cpd} — convection between waste package and drip shield
G_{rpd} — radiation between waste package and drip shield
G_{cdw} — convection between drip shield and drift wall
G_{rdw} — radiation between drip shield and drift wall

and for backfill (case 3)

$$Q_p = \left[G_{inv} + \left(\frac{1}{G_{cpd} + G_{rpd}} + \frac{1}{G_b} + \frac{1}{G_{cbw} + G_{rbw}} \right)^{-1} \right] \left(T_p - T_w \right) \tag{3}$$

where the effective conductance terms are defined to represent

G_b — conduction through the backfill
G_{cbw} — convection between backfill and drift wall
G_{rbw} — radiation between backfill and drift wall

As the drift degrades, G_b varies with the thickness of the rubble pile and G_{cbw} and G_{rbw} vary with the air gap distance between the rubble pile and the drift wall.

Inner drip shield temperature (T_d) and outer backfill temperature (T_b) can be calculated after the waste package surface temperatures have been estimated, using the following two expressions

$$Q_p - G_{inv}\left(T_p - T_w\right) = \left(G_{cpd} + G_{rpd}\right)\left(T_p - T_d\right) \tag{4}$$

and

$$Q_p - G_{inv}\left(T_p - T_w\right) = \left(G_{cbw} + G_{rbw}\right)\left(T_b - T_w\right) \tag{5}$$

Once temperatures across the in-drift environment have been calculated, effective thermal conductivity of air gaps can be estimated for use in porous media numerical models to represent radiative and convective heat transfer.

Effective thermal conductance terms for each case are presented next, organized by thermal process. Development of the equations follows the approach presented in Incropera and DeWitt (2002) and modified for Yucca Mountain emplacement drifts by Mohanty, et al. (2002) and a recently submitted proceedings paper.[1]

For conduction through the invert

$$G_{inv} = \frac{2\pi\left(1 - f_c\right)\left(L_p + 2\delta\right)k_f}{ln\left(\frac{D_w}{D_p}\right)} \tag{6}$$

where

π — 3.14…
f_c — fraction of waste package cylindrical surface available for convection and radiation
L_p — length of waste package
2δ — gap between waste packages
k_f — thermal conductivity of floor (invert) material
D_w — inner diameter of drift wall
D_p — outer diameter of waste package

For conduction through the backfill

$$G_b = \frac{2\pi f_c\left(L_p + 2\delta\right)k_b}{ln\left(\frac{D_b}{D_d}\right)} \tag{7}$$

[1]Mohanty, S., G. Adams, and J. Menchaca. “An Abstracted Model for Estimating Temperature and Relative Humidity in the Potential Repository at Yucca Mountain.” Proceedings of the 2004 ASME Heat Transfer/Fluid Engineering Summer Conference, Charlotte, North Carolina, July 11–15, 2004. New York City, New York: ASME. Submitted for publication (2004).

where

k_b — thermal conductivity of backfill material
D_b — outer diameter of backfill
D_d — diameter of drip shield, thickness assumed negligible

For convection, it is assumed the effective thermal conductivity (k_{nc}) value does not change with the temperature and the temperature difference for the gap over which convection is occurring. Thus, the same value of k_{nc} is used for convection from (i) the waste package to the drift wall, (ii) from the waste package to the drip shield, and (iii) the drip shield or backfill to the drift wall.

For convection

$$G_{cio} = \frac{2\pi f_c \left(L_p + 2\delta\right) k_{nc}}{ln\left(\frac{D_o}{D_i}\right)} \tag{8}$$

The subscripts for G_{cio} refer to convection, inner diameter, and outer diameter, where the diameters refer to waste package (p), drip shield (d), and drift wall (w) in Eqs. (1) through (3). The linearization of the k_{nc} to a constant value was assessed by Manepally, et al. (2003) and shown to be a reasonable assumption. Substitutions for G_{cio}, D_i, and D_o for specific legs of the thermal networks for each scenario [Eqs. (1) through (3)] are defined in Table 1.

For radiation

$$G_{rio} = \frac{\sigma\pi f_c\left(L_p + 2\delta\right)}{\frac{1}{D_i\varepsilon_i} + \frac{1}{D_o}\frac{1-\varepsilon_o}{\varepsilon_o}} 4T_w^3 \tag{9}$$

where

σ — Stefan-Boltzman constant
ε_i — emissivity of inner surface material (i.e., waste package and drip shield)
ε_o — emissivity of outer surface material (i.e., drip shield and drift wall)

The subscripts for G_{rio} refer to radiation, inner surface, and outer surface, where the surfaces are the waste package (p), drip shield (d), and drift wall (w). Similar to the convection substitutions, G_{cio}, D_i, D_o, ε_i, and ε_o for specific legs of the thermal networks for each scenario [Eqs. (1) through (3)] are defined in Table 1. The use of the drift wall temperature cubed in Eq. (7) is a linearization of the nonlinear radiation equation following the approach of Mohanty, et al. (2002). Equation (9), however, differs from that presented in Mohanty, et al. (2002) and a recently submitted ASME proceedings paper.[2] Equations (5-6) and (5-7) in Mohanty, et al. (2002) are written for radiation from one wall of an enclosure of general shape. Using the geometry of the emplacement drifts, the equations in Mohanty, et al. (2002) can be simplified to that shown in Eq. (9). For waste package to drift wall radiative-heat transfer, the linearization

[2]Ibid.

Table 1. Substitutions of Inner and Outer Diameters to Use for Eq. (8) (Convection) and Diameters and Emissivities to Use for Eq. (9) (Radiation) Depending on the Specific Leg of the Thermal Network						
Case	**Description**	**Effective Conductance G_{cio} or G_{rio}**	**Inner Diameter D_i**	**Outer Diameter D_o**	**Inner Emissivity ε_i**	**Outer Emissivity ε_o**
1 Preclosure	Waste package to drift wall	G_{cpw} or G_{rpw}	D_p	D_w	ε_p	ε_w
2 and 3	Waste package to drip shield	G_{cpd} or G_{rpd}	D_p	D_d	ε_p	ε_d
2 Backfill	Drip shield to drift wall	G_{cdw} or G_{rdw}	D_d	D_w	ε_d	ε_w
3 Backfill	Backfill to drift wall	G_{cbw} or G_{rbw}	D_b	D_w	ε_b	ε_w

assumes that, for example, $4T_w^3 \approx \left(T_w^2 + T_p^2\right)\left(T_w + T_p\right)$ for case 1. This linearization was assessed by Manepally, et al. (2003) and shown to be a reasonable assumption for the network algorithm approach.

The thermal network approach has the flexibility to assess the effect of the boundary condition imposed at the drift wall and the assumption of radial symmetry for the in-drift components. The sensitivity of these two assumptions was assessed in Fedors, et al. (2003) and Manepally, et al. (2003). The location of the boundary condition was seen to prominently affect in-drift temperatures for no degradation (case 2), but not for drift degradation (case 3). Sensitivity to asymmetry approximations was not significant.

To assess the effect of the boundary condition being placed at the drift wall, an additional leg that extends the network into the wallrock some specified distance can be added [Eq (10)],

$$Q_p = \left[\left(\frac{1}{G_{inv} + G_{rk}}\right)^{-1} + \left(\frac{1}{G_{cpd} + G_{rpd}} + \frac{1}{G_b} + \frac{1}{G_{cbw} + G_{rbw}} + \frac{1}{G_{rk}}\right)^{-1}\right]\left(T_p - T_{rk}\right) \qquad (10)$$

where the G_{rk} and T_{rk} refer to conductance and temperature for some distance into the wallrock. Although the addition of wallrock leg to the network does not eliminate the error in a priori specification of the outer boundary condition temperature for the in-drift heat-transfer algorithm, sensitivity analyses could be used assess the effect until process-level modeling is performed. Generally, moving the boundary condition farther from the integral portion of the problem domain lessens the effect of errors in the boundary condition value.

To assess the assumption of radial symmetry for the elliptical drift wall degradation and rubble pile buildup, a thermal network with three legs can be created: one for the conduction through the invert, a second for conduction laterally through the side of the drip shield and accumulated rubble, and a third vertically through the rubble pile and air space above the drip shield. A

geometric fraction for the second and third leg of the thermal network would be used to reflect the elliptical shape of the degradation (i.e., the fraction for the upward vertical leg could vary from 0.0 to 0.25 with the former representing no asymmetry). The rubble pile thickness would be constrained laterally by the un-degraded sidewall of the drift in the second leg of the network. The rubble pile thickness and drift ceiling height could continue to increase beyond the original drift diameter. Equation (11) represents thermal network for testing the effect of asymmetry; the fractions would be applied when estimating the conductance terms

$$Q_p = \left[G_{inv} + \left(\frac{1}{G_{cpd} + G_{rpd}} + \frac{1}{G_{b,t}} + \frac{1}{G_{cbw,t} + G_{rbw,t}} \right)^{-1} + \left(\frac{1}{G_{cpd} + G_{rpd}} + \frac{1}{G_{b,l}} + \frac{1}{G_{cbw,l} + G_{rbw,l}} \right)^{-1} \right] \left(T_p - T_{rk} \right) \quad (11)$$

where the *l* subscript refers to lateral heat transfer and *t* refers to vertically upward heat transfer. The terms inside the drip shield only vary by the fraction reflecting the elliptical shape. Outside the drip shield, the lateral leg of the thermal network initially has no rubble thickness, later has no air gap, and the rubble thickness constrained by the drift diameter.

REFERENCES

Fedors, R., S. Green, D. Walter, G. Adams, D. Farrell, and S. Svedeman. "Temperature and Relative Humidity Along Heated Drifts with and without Drift Degradation." CNWRA 2004-02. San Antonio, Texas: Center for Nuclear Waste Regulatory Analyses. 2004.

Fedors, R.W., G.R. Adams, C. Manepally, and S.T. Green. "Thermal Conductivity, Edge Cooling, and Drift Degradation—Abstracted Model Sensitivity Analyses for Yucca Mountain." San Antonio, Texas: Center for Nuclear Waste Regulatory Analyses. 2003.

Incropera, F.P. and D.P. DeWitt. *Fundamentals of Heat and Mass Transfer.* 5th Edition. New York City, New York: John Wiley and Sons. 2002.

Manepally, C., R. Fedors, G. Adams, and S. Green. "Effects of Drift Degradation on Environmental Conditions in Drifts." Fall Meeting Supplement, American Geophysical Union 2003 Fall Meeting, San Francisco, California, December 8–12, 2003. *Eos Transactions, American Geophysical Union*. Vol. 84, No. 46. 2003.

Mohanty, S., T.J. McCartin, and D.W. Esh. "Total-system Performance Assessment (TPA) Version 4.0 Code: Module Descriptions and User's Guide." San Antonio, Texas: Center for Nuclear Waste Regulatory Analyses. 2002.